Final Report for Research Conducted from July 1, 2006 to May 30, 2008

Award Number: DE-FC26-06NT42763

Recipient: PPG Industries, Inc., Glass Technology Center - R&D
400 Guys Run Rd., Cheswick, PA 15024

Project Title: Energy Efficient Electrochromic Windows Incorporating Ionic Liquids

Principal Investigator: Irina Schwendeman, PPG Industries Inc., Coatings Innovation Center
4325 Rosanna Dr., Allison Park, PA 15101
Phone: 412-492-5473, e-mail: ischwendeman@ppg.com

Project Manager: Adam Polcyn, PPG Industries, Inc., Glass Technology Center
400 Guys Run Rd., Cheswick, PA 15024
Phone: 412-820-4918, e-mail: apolcyn@ppg.com

John Winter, PPG Industries, Inc., Glass Technology Center,
400 Guys Run Rd., Cheswick, PA 15024
Phone: 412-820-8084, e-mail: jwinter@ppg.com

Business Contact: Brad Clawson, PPG Industries Inc., Coatings Innovation Center
4325 Rosanna Dr., Allison Park, PA 15101
Phone: 412-492-5165, e-mail: bclawson@ppg.com

Mike Lawless, PPG Industries, Inc., Glass Technology Center,
400 Guys Run Rd., Cheswick, PA 15024
Phone: 412-820-8572, e-mail: mlawless@ppg.com

PPG Contributors: Cheri Boykin, Lead Project Chemist-Glass Technology Center
James Finley, Consultant, Physicist-Glass Technology Center
Donald Anthony, Technician-Glass Technology Center
Julianna Knowles, Technician-Glass Technology Center
Richard Markovic, Technician-Glass Technology Center
Michael Buchanan, Engineering Consultant, Modeling and Simulations-Glass Technology Center
Mary Ann Fuhry, Chemist-Coatings Innovation Center
Lisa Perrine, Chemist-Coatings Innovation Center

DISCLAIMER

This Phase 1 Project Completion Report is structured according to the 7 items listed as requirements for the Final Scientific/Technical Report in the Federal Assistance Reporting Instructions (5/06) included with the Award. Items 1 and 2 are provided on page 1. The remaining items are provided in the following.

3. Executive Summary

One approach to increasing the energy efficiency of windows is to control the amount of solar radiation transmitted through a window by using electrochromic technology. What is unique about this project is that the electrochromic is based on the reduction/oxidation reactions of cathodic and anodic organic semi-conducting polymers using room temperature ionic liquids as ion transport electrolytes. It is believed that these types of coatings would be a lower cost alternative to traditional all inorganic thin film based electrochromic technologies. Although there are patents[1] based on the proposed technology, it has never been reduced to practice and thoroughly evaluated (i.e. durability and performance) in a window application.

We demonstrate that by using organic semi-conductive polymers, specific bands of the solar spectrum (specifically visible and near infrared) can be targeted for electrochemical variable transmittance responsiveness. In addition, when the technology is incorporated into an insulating glass unit, the energy parameters such as the solar heat gain coefficient and the light to solar gain ratio are improved over that of a typical insulating glass unit comprised of glass with a low emissivity coating. A minimum of ~0.02 quads of energy savings per year with a reduction of carbon emissions for electricity of ~320 MKg/yr benefit is achieved over that of a typical insulating glass unit including a double silver low-E coating. Note that these values include a penalty in the heating season. If this penalty is removed (i.e. in southern climates or commercial structures where cooling is predominate year-round) a maximum energy savings of ~0.05 quad per year and ~801 MKg/yr can be achieved over that of a typical insulating glass unit including a double silver low-E coating.

In its current state, the technology is not durable enough for an exterior window application. The primary downfall is that the redox chemistry fails to recover to a bleached state upon exposure to heat and solar radiation while being cycled over time from the bleached to the dark state. Most likely the polymers are undergoing degradation reactions which are accelerated by heat and solar exposure while in either the reduced or oxidized states and the performance of the polymers is greatly reduced over time.

For this technology to succeed in an exterior window application, there needs to be more work done to understand the degradation of the polymers under real-life application conditions such as elevated temperatures and solar exposure so that recommendations for improvements in to the overall system can be made. This will be the key to utilizing this type of technology in any future real-life applications.

[1] US6828062B2, US20020177039A1, EP1352111A1, EP1352111A4, WO2002063073A1: Long-Lived Conjugated Polymer Electrochemical Devices Incorporating Ionic Liquids
US6667825B2, US20020191270A1, EP1348045A1, EP1348045A4, EP1348045B1, WO2002053808A1: Stable Conjugated Polymer Electrochromic Devices Incorporating Ionic Liquids

4. Comparison of Actual Accomplishments with the Goals and Objectives of the Project

The goal of Phase 1 was to select the materials to be used in an electrochromic device (3 inch by 3 inch) that would eventually be scaled up for Phases 2 and 3 (12 inch by 12 inch and 24 inch by 36 inch, respectively). This selection was completed for the cathodic and anodic semi-conducting polymers, the electrolyte used for ion transport and the transparent conducting electrodes. In addition, a process was developed for depositing the transparent conductive electrodes onto glass substrates greater than 12 inches in one dimension. The system was also optimized for spectral performance, durability, energy performance and materials cost.

5. Summary of Project Activities

A list of all of the abbreviated terms used within this document is given in the Appendix.

For many years, coatings have been applied to windows in order to control the amount of solar radiation (ultraviolet, visible and infrared) admitted to a building. Coatings such as PPG's Solarban® 60 low-E coating transmit a high percentage of visible solar radiation, but block the ultraviolet and infrared components of the solar spectrum to prevent deterioration of furniture (due to UV) and reduce the heat load on the building (due to IR). Other glass products, such as PPG's GrayLite® glass, transmit low amounts of ultraviolet, visible and infrared radiation and provide the greatest reduction of solar load. However, none of these types of glass products provide dynamic control over the amount of solar radiation admitted. For example, while Solarban 60 reflects solar infrared radiation, it transmits a great deal of visible light, which building inhabitants may want to reduce to prevent glare. Also, while it is desirable to block infrared radiation during summer daylight hours to reduce energy expenditure for cooling, during winter daylight hours it may be desirable to admit infrared radiation to reduce energy expenditure for heating. The goal of this work is to develop a "smart" window that would allow control over the amount of solar visible light admitted to a building using an organic-based electrochromic device. The device consists of transparent inorganic conducting electrodes (TCOs), an organic semi-conducting polymer (OSCP) anode and cathode and a room temperature ionic liquid electrolyte (RTIL).

The anodically coloring semi-conducting polymer changes its color from light to dark when oxidized and from dark to light when reduced. The cathodically coloring polymer changes its color from light to dark when reduced and from dark to light when oxidized. The electrolyte serves as the ion reservoir providing the ions (anions and cations) required for the electrochemical redox reactions between the two polymer layers. Thus, transmittance of the assembled electrochromic device can be controlled between a bleached state and a darkened state (or any tint in between) by adjusting the voltage applied between the two polymer electrodes.

The overall performance of the OSCP electrochromic device is determined by the physical properties of both the polymers and the electrolyte. In the past, practical applications of all previous OSCP electrochromic windows have been limited by their short operational lifetimes with common degradation paths including side reactions with water and oxygen, evaporative loss

of electrolyte, and irreversible oxidation or reduction at high applied switching potentials.[2] Conventional electrolytes typically made by dissolving a solid ionic salt in a liquid solvent also play a critical role in contributing to these degradation problems. The use of water as a solvent (aqueous electrolyte) affects polymer electrochemical behavior and thus limits its use in window applications. The use of organic solvent electrolyte systems can partially solve these problems; however, most of the organic electrolytes studied are subject to absorption of water/moisture, and the organic solvent itself can evaporate.

RTIL electrolyte systems offer an advantage over that of conventional electrolyte systems in that they are intrinsically fluid over a wide temperature range (-100° to 500° C in several systems), require no solvent and exhibit high ionic conductivity (10^{-3} to 10^{-4} S/cm) with a wide range of electrochemical stability (-2.5 to +2.5 V). They are also non-volatile and non-flammable. These properties are very important for the fabrication of stable electrochromic windows that must tolerate extreme heat, cold and moisture exposure. SFST has demonstrated the application of RTILs as electrolytes with OSCP redox reactions[3] and has patents covering the use of RTILs within electrochromic cells.[4]

Typically, ionic liquids consist of nitrogen or phosphorus-containing organic cations and inorganic anions as shown in Figure 1 below. Critically, the mechanical and physical properties of ionic liquids can be tailored by modifying their chemical structure.

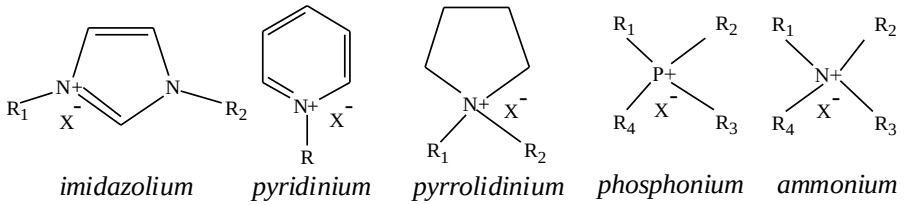

Figure 1. Structures of ionic liquids. Combination of different cations and anions results in various ionic liquids. R = methyl, ethyl, butyl, octyl, etc. X^- = BF_4^-, PF_6^-, $CF_3SO_3^-$, $(C_4F_9)_3PF_3^-$, etc.

The work covered within this document focuses on Phase 1 of the proposal with the objective of demonstrating a small electrochromic device incorporating conductive polymers and ionic liquid electrolytes that meets pre-established target levels for a glazing application. These include at a minimum, a contrast variation of greater than 40 percent between bleached and darkened states with a bleached state transmittance of greater than 50 percent, an aesthetically desirable bleached and darkened state color, uniformity of color over monolithic window surface such that ΔE_{cmc} is

[2] Schwendeman, I.; Hickman, R.; Sonmez, G.; *et al*; *Chem. Mater.* **2002**, *14*, 3118.

[3] (a) Lu, W.; Fadeev, A.G.; Qi, B.; *et al*; *Science* **2002,** *983*, 297.
(b) Lu, W.; Fadeev, A.G.; Qi, B.; Mattes, B.R.; *Syn. Metals* **2003,** *139***,** 135-136.
(c) "Ionic Liquids Boost Polymer Performance" *Chemical and Engineering News* **2002,** *26*, 80.

[4] US6828062B2, US20020177039A1, EP1352111A1, EP1352111A4, WO2002063073A1: Long-Lived Conjugated Polymer Electrochemical Devices Incorporating Ionic Liquids
US6667825B2, US20020191270A1, EP1348045A1, EP1348045A4, EP1348045B1, WO2002053808A1: Stable Conjugated Polymer Electrochromic Devices Incorporating Ionic Liquids

less than 3 MacAdam units for any 2 points on the window, coloration/decoloration switching time less than 2 minutes, contrast degradation and color uniformity changes less than 5 percent over 50,000 coloration/decoloration cycles. In addition, the device must pass durability testing following ASTM E2141-06 or NREL methods and commercial manufacturing costs should be defensibly estimated to be less than $100 per square foot. The results for each task required to accomplish the goals for Phase 1 are presented in the remainder of the document. A schematic of the device construction employed for this work is represented in Figure 2 below.

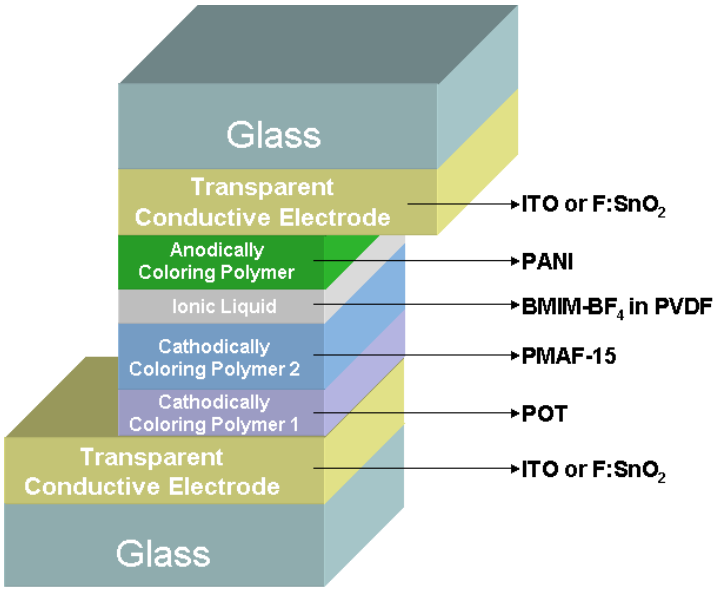

Figure 2. Schematic of the electrochromic device construction and stack sequences.

Task 1.0—Identify and Investigate Suitable Organic Semiconducting Polymers

The organic semiconducting polymers that were selected and investigated during the scope of this work included polyaniline (PANI) as the anodically coloring polymer and a combination of two cathodically coloring polymers: poly(3-octylthiophene-2,5-diyl) (POT) and poly(3,4-(2',2'-dimethylpropylene)-dioxythiophene) (PMAF-15). Unless noted otherwise, the ITO transparent conductor used in this work was purchased from Delta Technologies with a sheet resistance of 8 to 12 ohms per square. The dimensions were 25 mm by 75 mm by 1 mm.

Anodic Polymer. PANI is commercially available and was purchased from Ormecon GmbH as a nanodispersion in organic solvents (Product D1020). Ormecon reports that the conductivity of the polymer is 200 S/cm at 165 nm when the dispersion is spin coated for 5 seconds at 500 rpm and 3 seconds at 1500 rpm and allowed to dry at 100^{o}C for 1 minute. The nanodispersion was used as received. The optimized film deposition conditions were as follows: a 1.7 weight percent dispersion was spin coated at 5000 rpm for 10 seconds and the coated substrate was dried in vacuum oven at 65^{o}C at less than 40 mmHg for 16 to 18 hours.

During the optimization of the PANI layer, spectral data was collected for the PANI coated TCO glass by itself using BMIM-BF_4 as the electrolyte and a stainless steel plate as the counter

electrode with a silver wire as the reference electrode. When the PANI film thickness was increased by decreasing the deposition speed during spin coating, there was an increase in the near infrared and the visible transmittance noted when the voltage was cycled from -1.5 volts to +1.5 volts. At 5000 rpm (Figure 3A), there is some change in the visible transmittance (400-800 nm), but little change in the near infrared transmittance (800-1000 nm). At 3000 rpm (Figure 3B), there is more change noted in the near infrared region as a function of applied voltage and the largest difference in both the near infrared and visible regions is noted for the thickest film that was applied at 1000 rpm (Figure 3C); however, when the same films were incorporated into devices, the same effect was not observed (see Figure 4). The bleached state responses for a complete device in the visible and near infrared regions are similar for both the 5000 rpm applied PANI film and the 1000 rpm applied film. In addition, the opposite response of what was observed for the PANI films of varying thickness by themselves is observed for the PANI films of varying thickness incorporated into devices; in the near infrared region, the bleached state transmittance is always less than the dark state transmittance for the devices. It is believed that the other components in the device rather than the PANI are dominating the spectral response so that there is no observed near infrared switching effect from the PANI as a function of PANI thickness. Ultimately, the deposition conditions for the PANI were selected to minimize the film thickness for cost considerations.

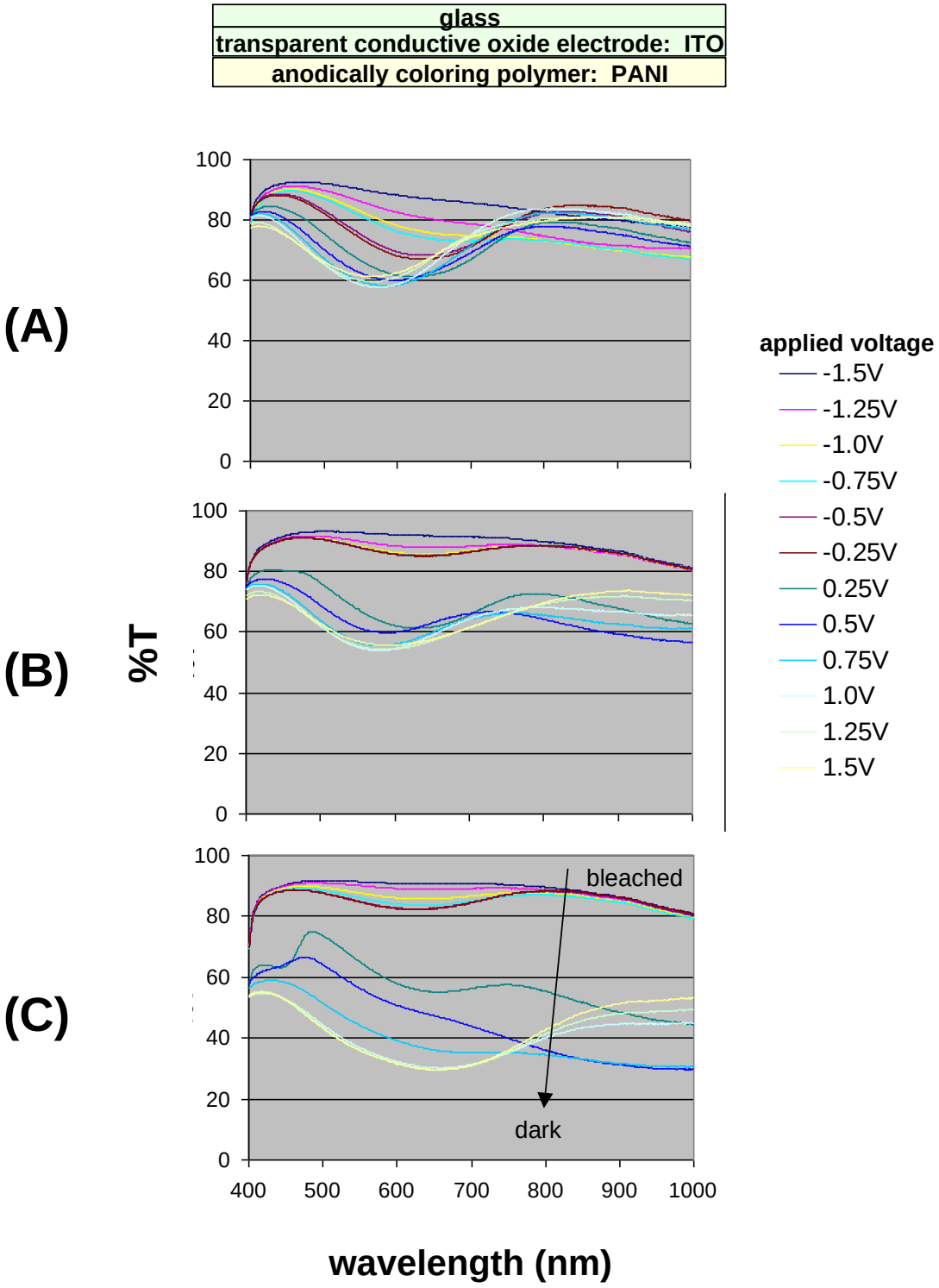

Figure 3. Transmittance spectra of PANI coated TCO glass with BMIM-BF_4 electrolyte, a silver wire reference and a stainless steel plate as the counter electrode as a function of applied voltage. 1.7 wt% PANI was deposited at different speeds to vary the film thickness: (A) 5000 rpm (B) 3000 rpm and (C) 1000 rpm. The 5000 rpm is the thinnest film and the 1000 rpm is the thickest film.

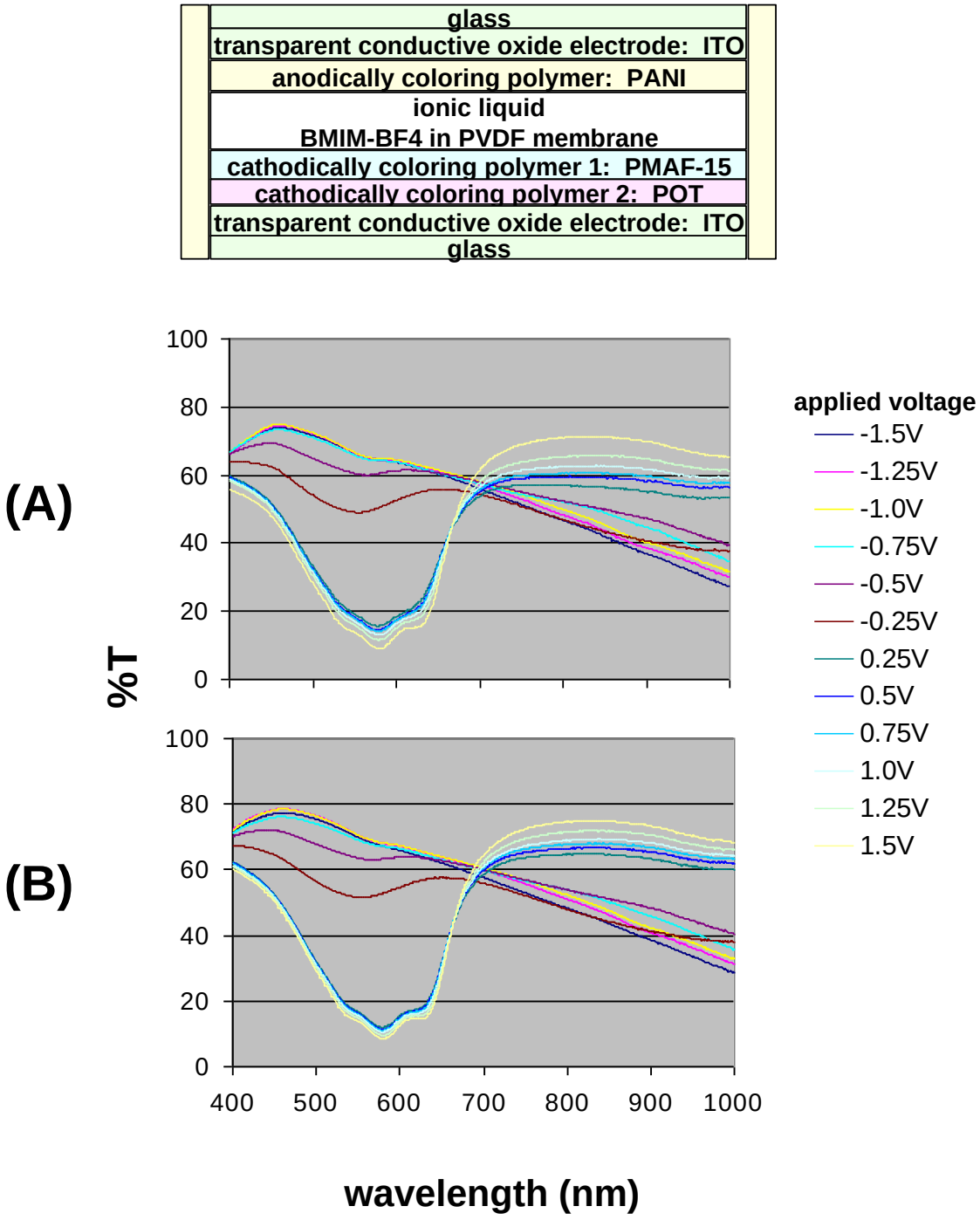

Figure 4. Transmittance spectra of electrochromic devices coated with two PANI thicknesses as a function of applied voltage. Stack configuration and materials noted in the schematic. 1.7 weight percent PANI was deposited at two speeds to vary the film thickness: (A) 5000 rpm and (B) 1000 rpm. The 5000 rpm is the thinnest film and the 1000 rpm is the thickest film corresponding to the same thicknesses in Figure 3A and 3C, respectively.

Cathodic Polymers. Two layers of cathodic polymers are used in this electrochromic device construction. The first, POT, was purchased from Reike Metals, Inc. (Product 4003E) and was used as received. The POT is required as a primer layer for the deposition of the PMAF-15 onto the TCO coated glass and contributes little to the electrochromism of the system. Ultimately, the deposition conditions for the POT were optimized to yield a uniform deposition of the second cathodic layer and to minimize the overall device cost. The polymer was dissolved in reagent grade toluene to 0.25 weight percent solids and was spin coated onto TCO coated glass substrates at 1000 rpm for 4 seconds and 2500 rpm for 30 seconds. The polymer coated glass was then dried in a vacuum oven at 65^{o}C at less than 40 mmHg for 16 to 18 hours.

Initially, poly(2,3-dihydrothieno[3,4-b]-1,4dioxin) (PEDOT)[5] was optimized for the cathodic layer. However, because a desired contrast of 40 percent or greater with a bleached state transmittance above 50 percent could not be achieved with this polymer combination (PANI/PEDOT/POT) within the electrochromic device, work focused on developing a new cathodic polymer in-house. A large portion of time was spent on synthesizing a new cathodic monomer that could be electrodeposited (MAF-15) and evaluating the contrast and durability of devices including this polymer (PMAF-15).

Devices containing the PMAF-15 showed not only a higher contrast than electrochromic devices containing PEDOT, but also a broader absorption peak covering more of the visible spectrum and giving the electrochromic devices a deeper darker color (see Figure 5). The PMAF-15 has almost no color in the oxidized state and therefore in the bleached state the devices approach the high transmittance of ITO coated glass alone. The maximum absorption of the new devices was shifted to 570 nm, as compared to 620 nm for the PEDOT based devices (see Figure 5 for the minimum transmittance). This is closer to the wavelength of maximum sensitivity for the human eye (555 nm), giving an electrochromic window an even higher perceived contrast which is more effective for shading. It is believed that the high contrast of PMAF-15 is due to a more open structure allowing the dopant ions to more easily go in and out of the polymer film.

Because promising durability results were obtained with these devices, a toll manufacturer was contacted and the material was successfully scaled up. Coincidentally, a few months after this material was scaled up at the toll manufacturer, it became commercially available through Aldrich (Product 660523: 3,4-(2',2'-dimethylpropylene)-dioxythiophene). Both the Aldrich Product and the toll manufactured materials behaved similarly and were used interchangeably for the electrochromic device performance and durability studies.

[5] PEDOT was electrodeposited from poly(2,3-dihydrothieno[3,4-b]-1,4-dioxin). This polymer is also commercially available from H.C. Starck under the family of Baytron ® Conducting Polymers.

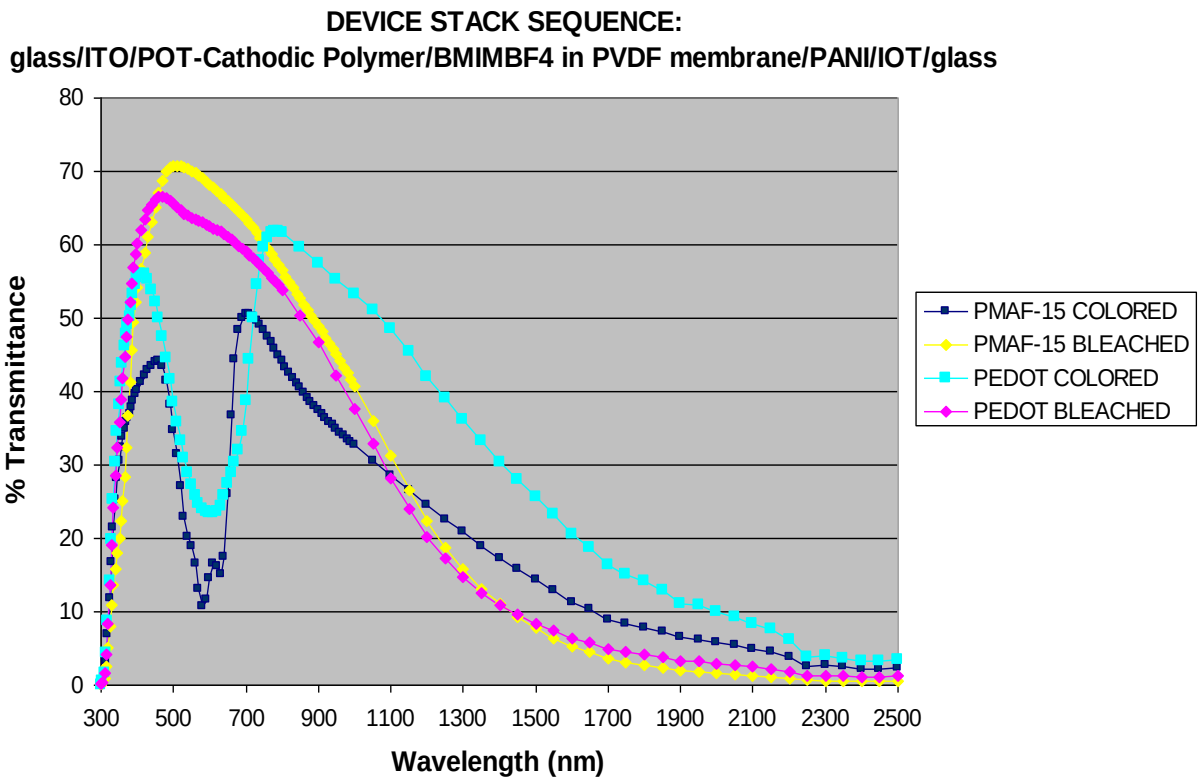

Figure 5. Transmittance spectrum comparing devices constructed with PMAF-15 versus PEDOT.

PMAF-15 was electrodeposited onto the POT coated TCO glass substrates. The electrodeposition conditions for the MAF-15 monomer were optimized for contrast and PTR with the goal of maintaining the transmittance of the device in the bleached state above 50 percent while minimizing the transmittance in the colored state.[6] This was achieved by varying the deposition thickness of the PMAF-15. PMAF-15 was electrodeposited onto POT-ITO coated glass from a solution of MAF-15 in 0.1 M TBAP in acetonitrile in a cell constructed to minimize solvent volume. The counter electrode was a stainless steel plate with a silver wire as the reference electrode. The PMAF-15 was grown until a charge of 0.5 to 1.0 C was achieved. With the variable film thicknesses, devices were constructed ranging from approximately 56 to 45 percent transmittance in the bleached state with approximately 8 to 2 percent transmittance in the colored state with PTRs ranging from 3.8 to 8.2 (see Figure 6). As the percent transmittance in the colored state is lowered, a more dramatic effect is observed in the response to the PTR relative to the PTR response for the bleached state.

[6] Recommendation from ASTM E2141-06 "Standard Test Methods for Assessing the Durability of Absorptive Electrochromic Coatings on Sealed Insulating Glass Units".

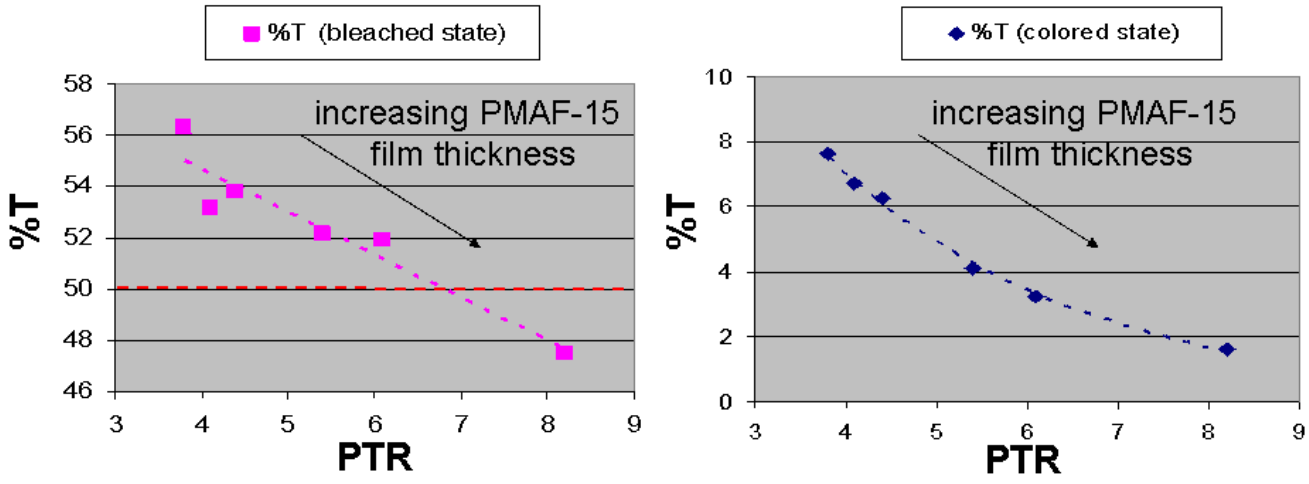

Figure 6. PMAF-15 Optimization: transmittance data taken at 582 nm for bleached and colored states as a function of increasing PMAF-15 film thickness. Device stack sequence is glass/ITO/POT/PMAF-15/BMIM-BF_4 in PVDF membrane/ PANI/ITO/glass.

The work discussed in Subtasks 1.1-1.3 contains additional approaches to increase the energy performance of the electrochromic IGU over that of the general approach that was outlined in the original contract. Two alternative OSCP devices were explored (multilayer devices and near infrared switching polymers), hybrid devices were investigated (WO_3) and a brainstorming session was held to propose novel approaches to increase the energy savings potential.

Subtask 1.1—Investigate New OSCP Devices

Multilayer Devices. A process to deposit multilayer cathodes of PEDOT/PMAF-15 was developed to see whether multiple OSCPs covering multiple regions of the solar spectrum could be incorporated into a single device. The stack sequence is as follows: glass/ITO/PANI/BMIM-BF_4 in PVDF/PMAF-15/PEDOT/POT/ITO/glass. For the multilayer electrodeposition, PEDOT was electrodeposited first from a solution of EDOT, then the substrate was rinsed and the solution replaced with MAF-15 monomer and PMAF-15 was electrodeposited onto the PEDOT coated substrate. This electrodeposition sequence was followed because the PEDOT seems to have better adhesion to bare ITO/glass than PMAF-15. PEDOT was also more conducting in the clear form, allowing for a better PMAF-15 deposition.

Table 1 shows the charge at which the deposition of each monomer was terminated and Figure 7 shows the spectral data for the devices in the dark state.

Table 1. Deposition Parameters		
	Termination Charge (C)	
Device	EDOT	MAF-15
1	0.50	----
2	0.30	0.20
3	0.20	0.30
4	0.20	0.30
5	----	0.50

A slight shoulder is noted at approximately 650 nm for the devices as the PEDOT thickness is increased. Because this peak is observed, we believe that it is possible to have devices with multiple absorption peaks throughout the visible and near infrared if the appropriate polymers were synthesized. We also believe that using multilayer stacks is a viable way to control transmission through various regions of the solar spectrum.

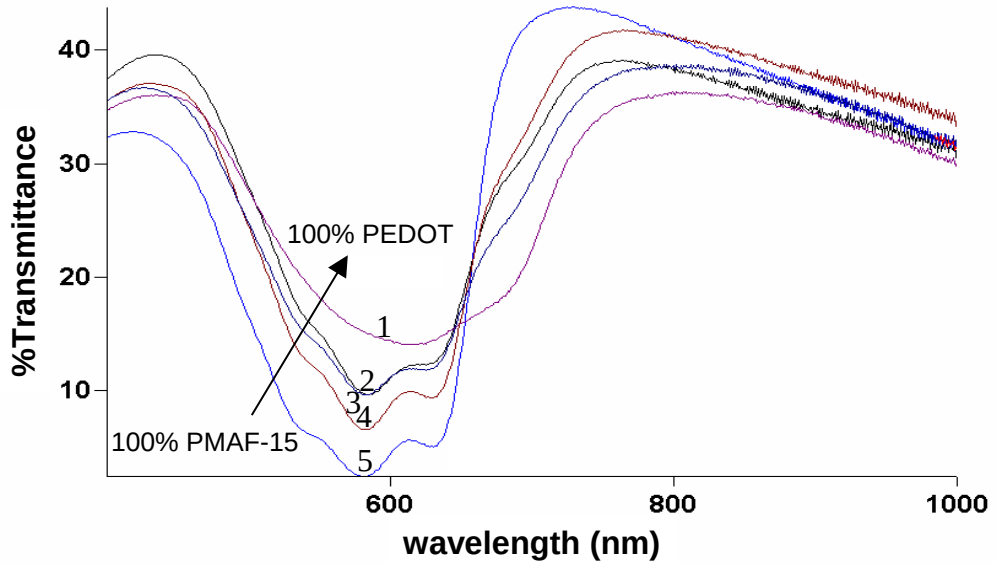

Figure 7. Devices ranging in PMAF-15 and PEDOT concentration. Dark state, +1.5 V applied. Relative concentrations are given in Table 1.

Near Infrared Switching Polymers. Contact was made with an outside supplier and several polymers were provided for screening. When one of the polymers was drop cast onto ITO coated glass and the spectral properties evaluated using a stainless steel plate as the counter electrode and silver wire as the reference electrode in propylene carbonate with 0.1M TBAP, electroactive transmittance in the near infrared region was noted as shown in Figure 8. When the polymer was in the oxidized state, little to no near infrared transmittance was observed and when the polymer was in the reduced state, as much as 73 percent transmittance was observed. These results demonstrate that variable infrared properties can be achieved; however, this particular polymer would not be suitable for shading as there is low visible transmittance in both the reduced and oxidized states.

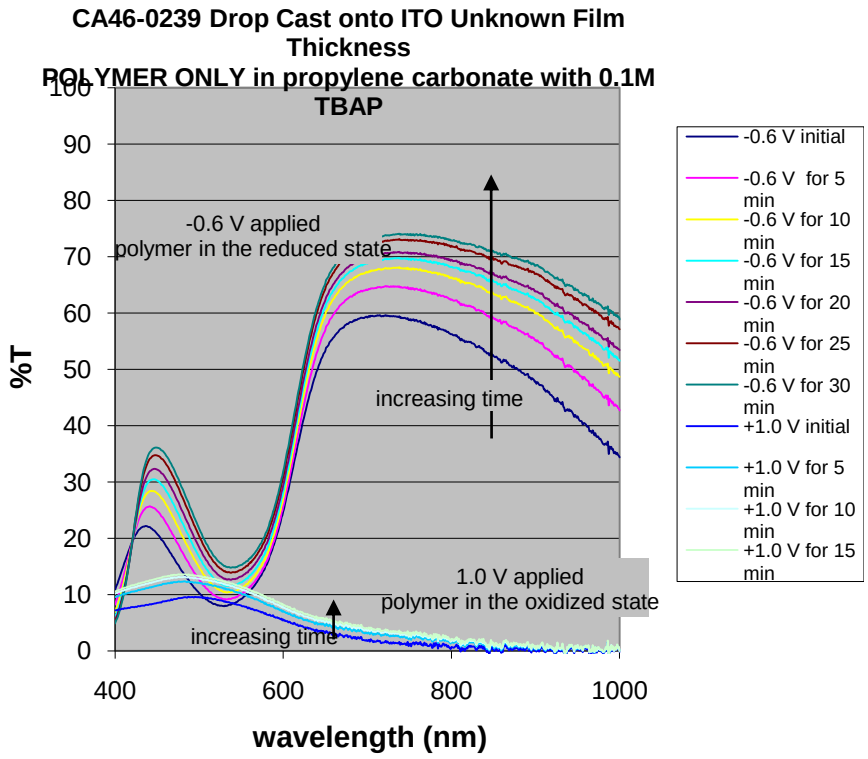

Figure 8. Transmittance data for a NIR electroactive polymer in the oxidized (+1.0 V applied) and reduced states (-0.6V applied). The electrolyte is 0.1M TBAP in propylene carbonate.

When the same polymer was incorporated into an electrochromic device, the electroactive polymer did not reduce the transmittance in the near infrared region to less than 10 percent transmittance as was observed for the polymer by itself. Figures 9-11 demonstrate this effect when a variety of electrolytes were used within the cells.

When the electrolyte within the device was kept the same as with the half cell containing only the near infrared electroactive polymer film on ITO (TBAP in propylene carbonate—Figure 10), only minimal switching was noted from the NIR electroactive polymer at 1000 nm and effectively no switching was noted in the visible region from the PMAF-15. When the electrolyte was changed to TBAP in BMIM-BF_4, switching improved in the visible region from the PMAF-15 (approximately 20 percent); however, no additional switching was noted for the near infrared absorbing electroactive polymer. When the TBAP was removed and only BMIM-BF_4 was used as the electrolyte, the PMAF-15 contrast improved to approximately 25 percent, but the contrast in the near infrared region was still low at only 15 percent.

Although this particular polymer system exhibited only partial reversibility in these devices and conditions, our external supplier has developed other polymers within the same class that have been shown to be more completely reversible, and exhibit significant infrared dynamic response. Successful use of conjugated polymers in a dual device

should be possible with additional engineering of the device construction and composition, as well as possibly modification of the solubility/swellability properties of this or other polymer materials.

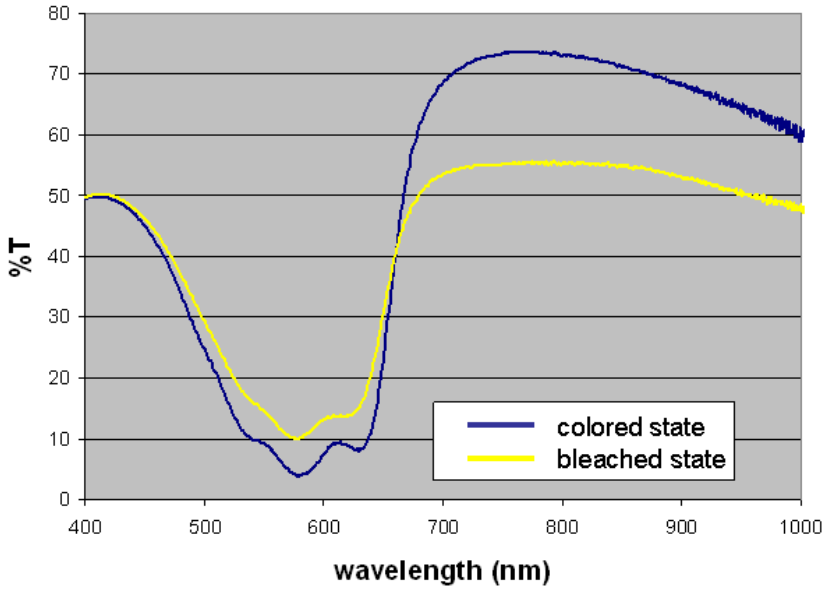

Figure 9. Transmittance data for a NIR electroactive polymer within a device of the following stack sequence: ITO/POT/MAF-15/PVDF membrane soaked in TBAP in propylene carbonate/NIR electroactive polymer/ITO. Applied voltage = ± 1.5V.

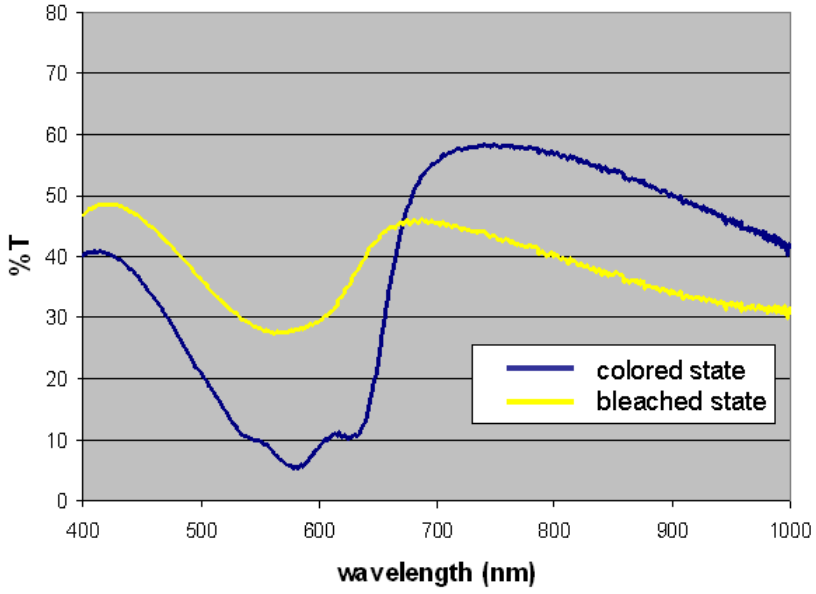

Figure 10. Transmittance data for a NIR electroactive polymer within a device of the following stack sequence: ITO/POT/MAF-15/PVDF membrane soaked in TBAP in BMIM-BF_4/NIR electroactive polymer/ITO. Applied voltage = ± 1.5V.

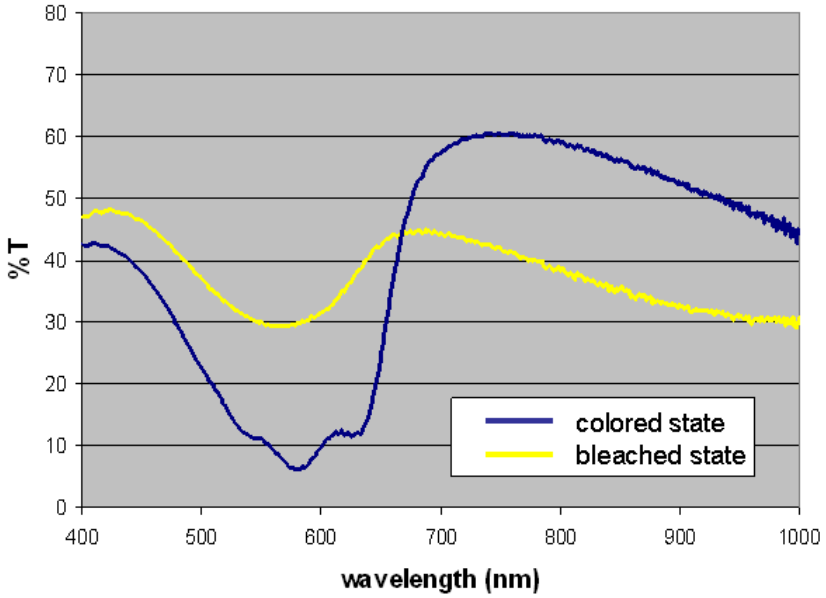

Figure 11. Transmittance data for a NIR electroactive polymer within a device of the following stack sequence: ITO/POT/MAF-15/PVDF membrane soaked in BMIM-BF_4/NIR electroactive polymer/ITO. Applied voltage = ± 1.5V.

The results from these studies are significant in that they do show that addressable infrared transmittance is possible. If future work is to be conducted in this area, polymer engineering will be required to achieve variable transmittance in the desired transmittance regions when the polymer is incorporated into electrochemical devices. In addition, a proper electrolyte that will allow the near infrared region electroactive polymer to switch within a device will need to be found and the durability of the entire system evaluated.

Another near infrared switchable polymer that was investigated was purchased from Aldrich (product number 482552). This material showed poor adhesion to the ITO and had minimal contrast between the colored and bleached states.

Subtask 1.2—Investigate Hybrid Devices

One approach for an organic/inorganic electrochromic hybrid device would be to incorporate tungsten oxide (WO_3) into the film stack. The challenge in working with this inorganic material is to reduce the electrochromic switching voltage of the WO_3 to a level that is low enough so that the organic polymers within the system do not degrade with the applied potential. Using WO_3 within the film stack would provide the broad band switching capability of the WO_3 plus the narrow band switching capability of the OSCP. To explore this approach, WO_3 films were prepared by MSVD of the film on ITO coated glass. Figure 12 shows the spectral data for a stack configuration including WO_3 as the cathodic layer and PANI as the anodic layer. A high potential (±4.0 V) was required before any switching was observed which led to irreversible damage of the electrochemical cell.

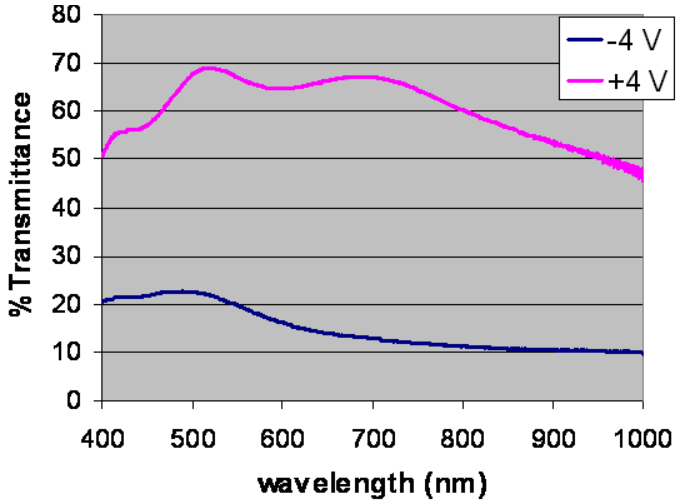

Figure 12. Stack configuration: glass/ITO/MSVD WO_3/BMIM-BF_4 in PVDF membrane/PANI/ITO/glass. ±4.0 V applied. PTR = 3.51.

When PEDOT was electrodeposited over the WO_3, the switching potential was reduced to ±2.8 V (see Figure 13). The PTR[7] of the devices was 3.5 and 3.3, respectively which is similar to that of the devices which did not contain tungsten oxide. Although the OSCP approach and the hybrid approach produce very different spectral data, most notably in the near infrared region, the similarity in the PTR is due to the fact that the PTR is weighted towards the visible response of the eye and not towards the infrared region of the solar spectrum.

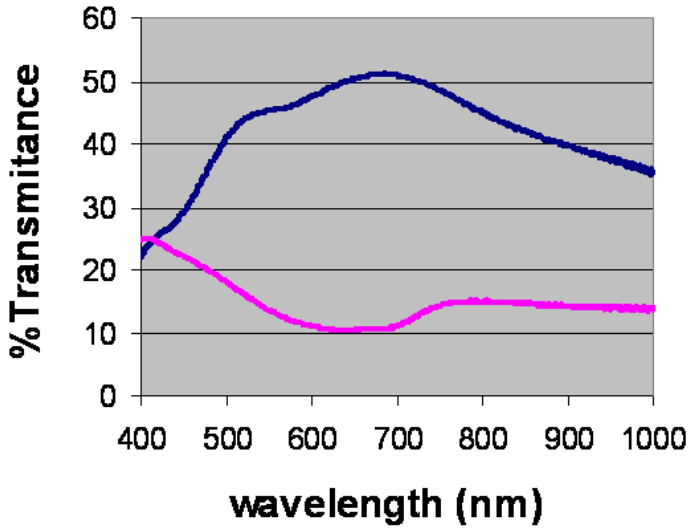

Figure 13. Stack configuration: glass/ITO/MSVD WO_3/PEDOT/BMIM-BF_4 in PVDF membrane/PANI/ITO/glass. ±2.8 V applied. PTR = 3.31.

Additional work would still need to be conducted in this area to further reduce the

[7] See ASTM 2141-06 for calculation of PTR value. ASTM 2141-06 also references the following regarding PTR: (1) R. Kingslake, "Applied Optics and Optical Engineering," in Vol. 1, *Light: Its Generation and Modification*, Academic Press, New York, NY, 1965, Table II, Chapter 1. (2) E1423 (3) C 1199 and (4) CAN/CGSB 12.8

switching voltage of the tungsten oxide to one more compatible with the organic polymers and to optimize the OSCP so that it contributes more towards the darkening of the device so a better contrast could be achieved. Ultimately, it would be preferred to be able to switch the organic and inorganic films independently, perhaps at different voltages which may be achievable with this approach due to the greater differences the redox potentials between the inorganic and organic films.

Subtask 1.3—Investigate Novel Approaches

A brainstorming session was held regarding infrared switching and increased energy savings. Some of the categories identified included: addition of low-E coatings to the IGU configuration, addition of infrared reflective polymers to the electrochemical stack, altering the ionic liquid, hybrid devices and thermotropic materials. Several of the approaches are being addressed in the current research.

Task 2.0—Investigate Ionic Liquid Electrolytes

Limited work was performed with the ionic liquids. This work focused on identifying an ionic liquid that was an effective electrolyte for the OSCPs identified in Task 1, had a melting/freezing point below that of a window application and was compatible with a membrane (i.e. high transparency and low haze) that could act as a spacer for the system. Eight membranes and seven ionic liquids were screened by our subcontractor SFST and are given in Tables 2 and 3 below.

Table 2. Membranes Screened for Dielectric Transport Layer

	Trade Name	Description	Material No.
1	GE MicronSep	Cellulosic	1215305
2	GE Polysep	Polypropylene	1214236
3	GE Poretics	Polycarbonate	1215303
4	GE Micron-PES	Polysulfone	1215368
5	GE AcetatePlus	Acetate	1212375
6	GE Poretics	Polyester	1220702
7	Millipore, Immobilon FL	Polyvinyladinefluoride, PVDF	---
8	Gore 0.5 mil PTFE	Polytetrafluoroethylene, PTFE	---

Table 3. Ionic Liquids Screened for Compatibility with Membrane Materials		
	Compound/Abbreviation	**Melting/Freezing Point (^{o}C)**
1	1-butyl-3-methylimidazolioum tetrafluoroborate $[BMIM]^{+}[BF_4]^{-}$	< -20
2	1-butyl-3-methylimidazolioum thiocyanate $[BMIM]^{+}[SCN]^{-}$	< -20
3	1-butyl-3-methylimidazolioum hexafluorophosphate $[BMIM]^{+}[PF_6]^{-}$	< -20
4	1-butyl-3-methylimidazolioum $[BMIM]^{+}[BF_6]^{-}$	< -20
5	1-butyl-3-methylimidazolioum methyl sulfate $[BMIM]^{+}[MeSO_4]^{-}$	< -20
6	1-methyl-3-octylimidazolium hexafluorophosphate $[OMIM^{+}][PF_6]^{-}$	- 88
7	1-ethyl-3-methylimidazolium bis(trifluoromethylsulfonyl) imide $[EMIM^{+}][TFSI]^{-}$	- 21

For a majority of the membranes (1-6), the combination of the membranes with the ionic liquids yielded an opaque result. The exception being that the $[BMIM]^{+}[SCN]^{-}$ and the $[BMIM]^{+}[MeSO_4]^{-}$ dissolved the GE MicronSep Cellulosic membrane. The only membranes that yielded some transparency in combination with the ionic liquids were the Millipore, Immobilon FL and the Gore 0.5 mil PTFE membranes (7-8) as shown in Figures 14 and 15 below. The Millipore membrane yields the highest transmittance and has much lower haze relative to that of the Gore membrane when soaked in $[BMIM]^{+}[BF_4]^{-}$.

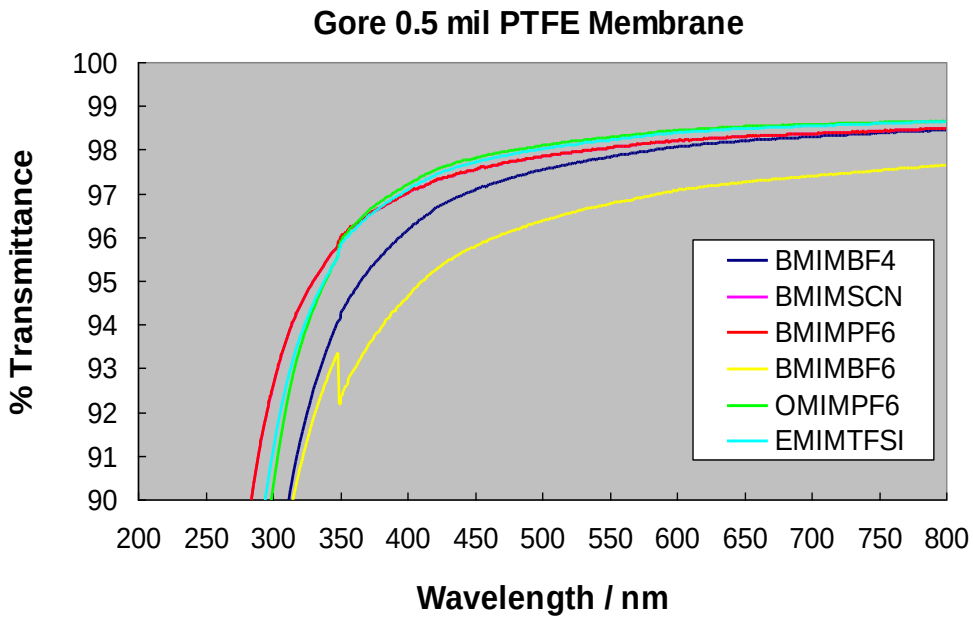

Figure 14. Transmission curves for Gore membrane soaked in various ionic liquids.

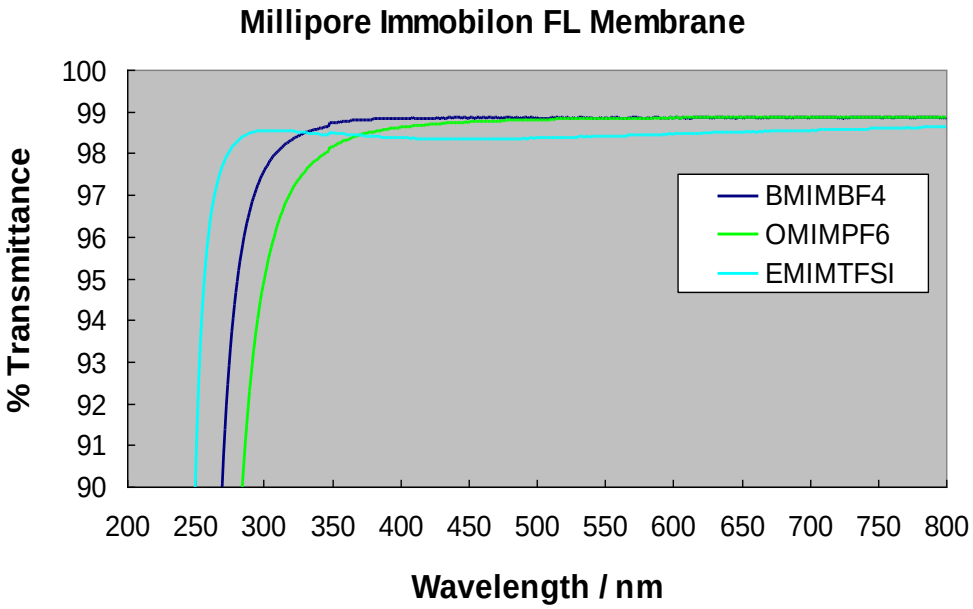

Figure 15. Transmission curves for Millipore membrane soaked in various ionic liquids. Note: Data was unavailable to plot for the $BMIM^+$ PF_6^- and $BMIM^+$ BF_6^- soaked membranes, although SFST reports that the $BMIM^+$ PF_6^- soaked membrane yields less than 6% loss in transmittance and the $BMIM^+$ BF_6^- soaked membrane yields less than 3% loss in transmittance over a majority of the transmittance spectrum.

PPG has focused on using $[BMIM]^+[BF_4]^-$ with the Millipore Immobilon FL PVDF membrane.[8] Analytical testing was performed to assess the UV stability of the ionic liquids after 67 and 235 hours of exposure to UVA-340 illumination. The samples were analyzed by IR, CNMR, HNMR and FNMR techniques. The analysis did not detect significant changes in the samples.

Task 3.0—Investigate Transparent Conducting Oxide Electrodes

An ITO coating was developed for use in an electrochromic cell consisting of conductive polymer electrodes and an ionic liquid. ITO coatings were deposited on a clear float glass substrate from a ceramic ITO target by planar magnetron sputtering in an oxygen-argon gas mixture. The amount of oxygen in the gas composition was varied between 2 and 20 percent. The ITO coated substrates were heated over a range of temperatures after deposition. Two ceramic targets, one worn and one new were compared. Operating parameters were then determined to deposit a coating with optimized properties for resistivity and transmittance. In addition, the coating thicknesses and substrate temperatures necessary to attain maximum transmittance at a sheet resistance of 10 ohms per square or less were calculated from the results of data.

The ITO coating was developed in an inline sputtering system that is capable of coating substrates up to 14 inches by 14 inches square using 5 inch by 17 inch cathode targets. Two targets were compared; one was partially worn, while the other target was new. The data presented here will focus on the coatings sputtered from the worn target. The comparison of properties between the targets was made to illustrate any differences in coating properties and deposition performance. The composition of the ITO ceramic target nominally contains 10 percent tin with the balance consisting of indium oxide. 12 inch by 12 inch by 2.3 mm thick clear float glass manufactured by PPG Industries was used as the coating substrate. The sheet resistance and transmittance of the coatings were measured both after deposition and post heating. Transmittance was measured using a BYK Gardner TCS Spectrophotometer, and sheet resistance was measured using an Alessi CPS-05 Contact probe station and a Kiethley 2010 multimeter. X-Ray Fluorescence (XRF) was used to determine the composition of the coating, and to set up a calibration curve for subsequent thickness measurements. Direct measurements of thickness were made using a Tencor stylus profilometer.

Three sets of samples were produced resulting in four data sets for coating properties both after deposition and after heating to 150, 200 and 250°C after deposition. Each set was run at six gas compositions with oxygen gas contents of 2, 4, 5, 7, 10 and 20 percent with argon making up the balance of the sputtering gas. Gas pressure was kept constant during deposition. Coating thickness and composition were measured for each sample after deposition. The deposition rate was determined from the coating thickness at a preset power, line speed and number of passes and expressed in terms of Angstroms per kW-pass. Sheet resistance and visible light transmittance were measured for each sample both after deposition and after post heating. Coating resistivity was calculated from the results of the thickness and sheet resistance measurements and expressed in terms of Ohm-Angstroms (not conventional but easy to convert from measured units). The thickness required for a sheet resistance of 10 ohms per square or less was calculated from the resistivity.

[8] $[BMIM]^+[BF_4]^-$ was purchased from EMD Chemicals as product 4.91049 and was used as received.

Figure 16 shows the deposition rate of the coating deposited from the worn target over the entire range of gas composition. The rate decreases after reaching about 5 percent oxygen gas content, indicating the approach of a smooth transition region from a more metallic target surface to a more oxidized and insulating surface with increased oxygen. The percentage of tin in the target composition also abruptly increases after 5 percent oxygen gas content. Although the target was run for only brief periods at a time, it is expected the target will eventually reach equilibrium composition.

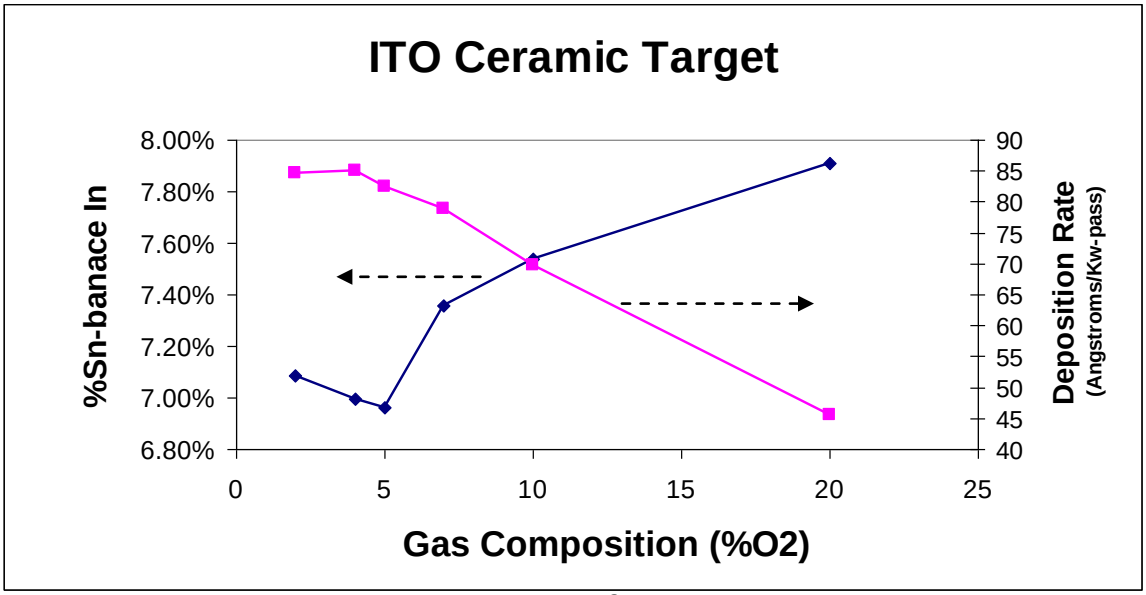

Figure 16. Composition and deposition rate for worn target. Deposition rate decreases with increasing oxygen content above 5 percent.

Figure 17 shows the behavior of resistivity after deposition as a function of the percentage of oxygen gas content. Each data point is an average of the resistivity after coating deposition from a set of samples to be post heated. The resistivity at 20 percent oxygen gas content was off-scale and is considered electrically insulating for this application, and therefore was not include in the figure. As the percentage of oxygen gas content increases, the coating becomes more oxidized and approaches a minimum in resistance, but any increase in oxygen beyond this minimum results in higher resistivity. The range of oxygen gas content for low resistivity films falls between 4 and 6 percent, with the optimum percentage around 5 percent. The resistivity increases dramatically when the percent of oxygen gas is above 7 percent. As illustrated in the chart, an increase of only 3 percent over the optimum percentage of oxygen gas content results in a 40 times increase in resistivity.

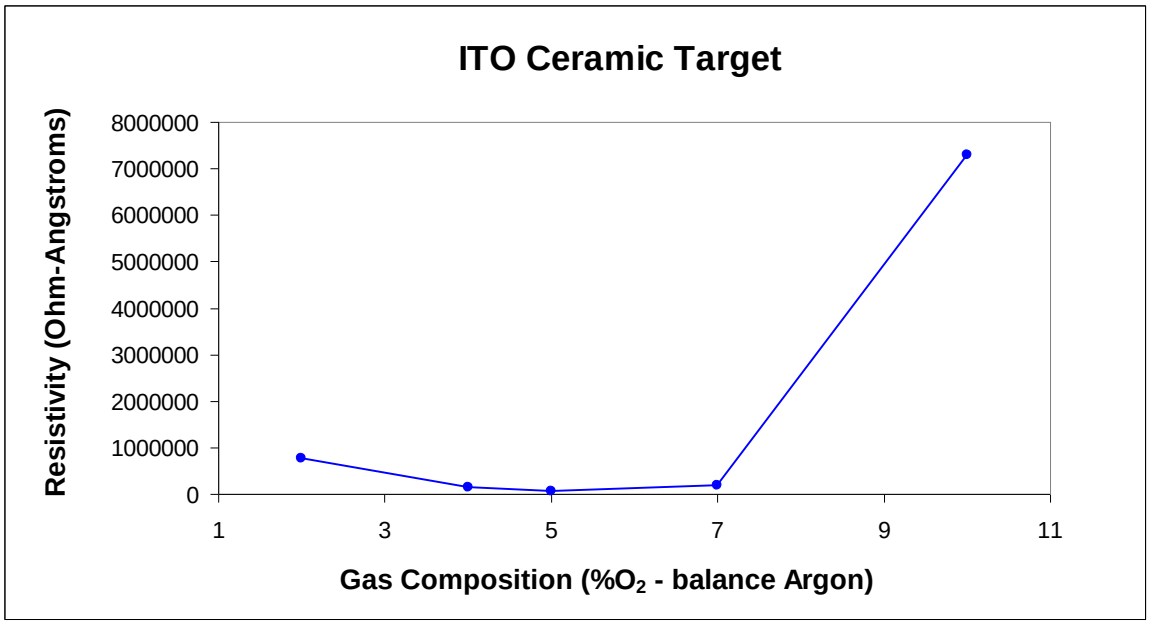

Figure 17. ITO film resistivity as a function of sputter gas composition.

Figure 18 shows the resistivity of the coatings for room temperature (after deposition) and three post heating temperatures for oxygen gas content in the region of interest, ranging from 4 to 7 percent. The chart clearly illustrates the minimum in resistance at 5 percent oxygen gas content at all three temperatures. As expected, the post heating improves the coating resistivity and does not change the position of the minimum resistivity. However, any increase above 200°C has no beneficial effect.

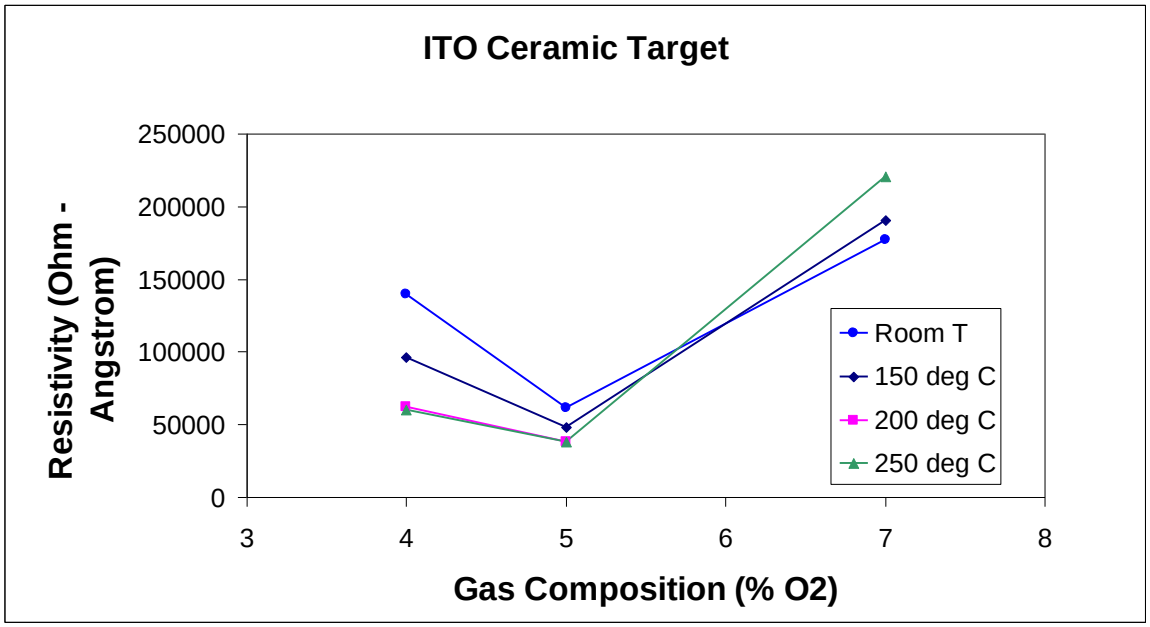

Figure 18. ITO coating resistivity as function of gas composition for various post-deposition heating temperatures.

The behavior of the transmittance with change in the percentage of the oxygen gas content is shown in Figure 19. Substrates post-heated to 200°C and above attain a maximum transmittance of about 87 percent for oxygen content greater than 5 percent. Substrates heated to 150°C attain a transmittance of only 80 percent at 5 percent oxygen gas content, with a maximum transmittance of around 85 percent for 7 percent oxygen gas content. Any increase in the temperature above 200°C does not have a beneficial effect. Figure 20 illustrates the behavior of the transmittance as a function of temperature.

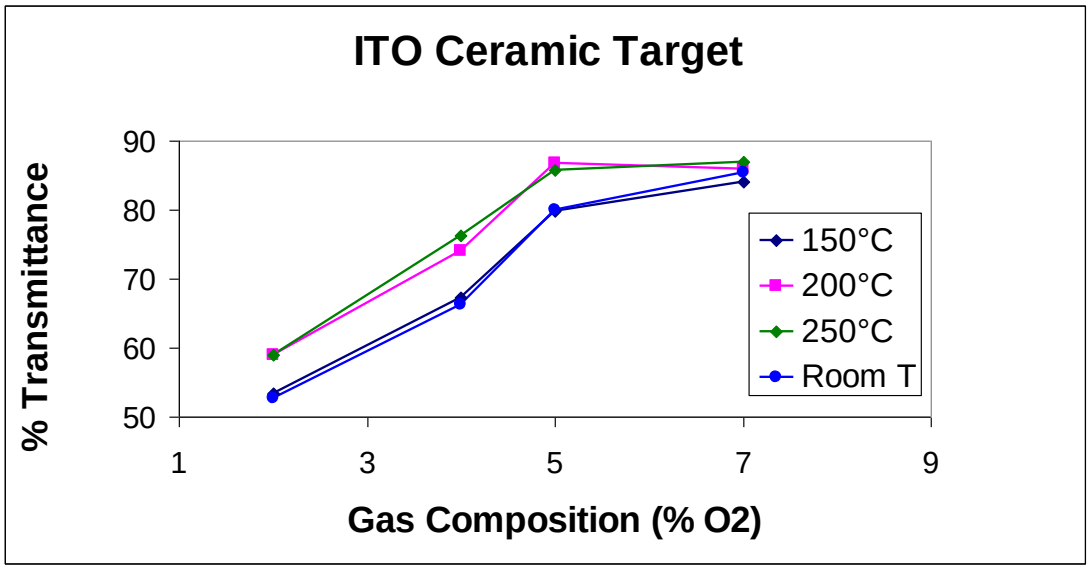

Figure 19. Transmittance as function of post-deposition heating temperature for various sputter gas (% O_2) compositions.

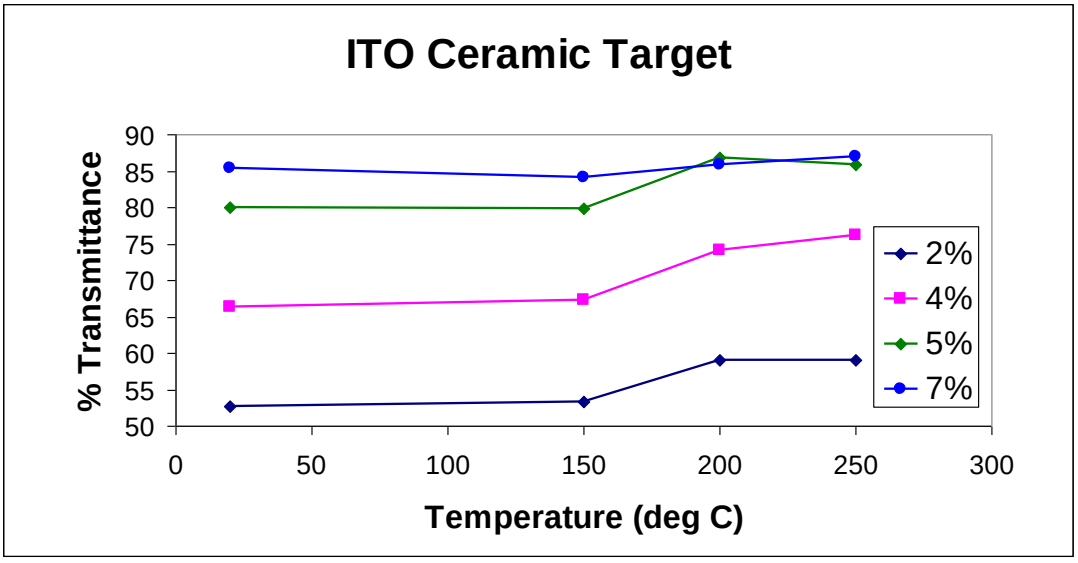

Figure 20. Optical transmittance as function of gas composition for various post-deposition heat treating temperatures.

The data for the worn target in Figures 18 and 19 indicate that when the substrate is heated to at least 200°C and the percentage of oxygen in the gas composition is set at 5 percent, both minimum resistivity and maximum light transmittance will be attained and deposition rate remains high.

A new ceramic ITO target was installed and the procedure was repeated to compare with the worn target. As shown in Figure 21 and 22, the trends for coating composition, resistivity, and transmittance as a function of gas composition are similar for the old and new targets; however there is an offset in the percentage of oxygen between targets which yields optimum coating composition. Figure 21 indicates that the optimum in resistivity after deposition is attained at 8 percent for the new target, or 3 percent higher than the percentage of oxygen for the old target. The deposition rate and transmittance (not shown) are also essentially equal for both targets, but shifted 3 percent higher for the new target. Figure 22 indicates that percentage of tin follows the same curve for both the new and old targets at the higher percentages of oxygen, however, the percentage of tin is higher for the new target at lower percentages of oxygen. It was determined that this small difference does not influence the properties of the coating.

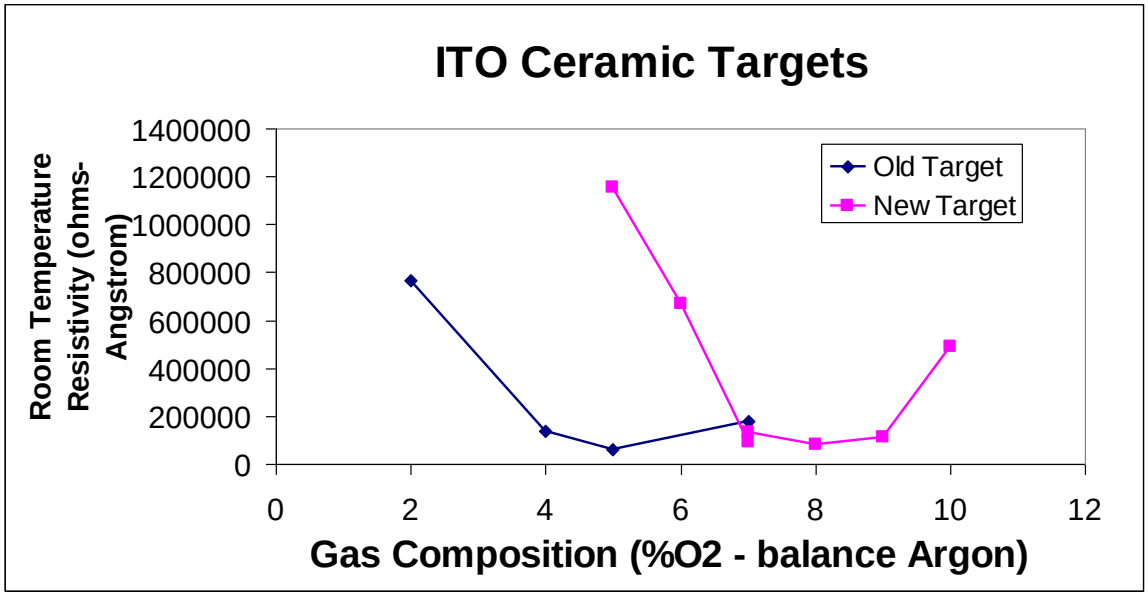

Figure 21. Comparison of resistivity as function of sputter gas composition for old and new targets.

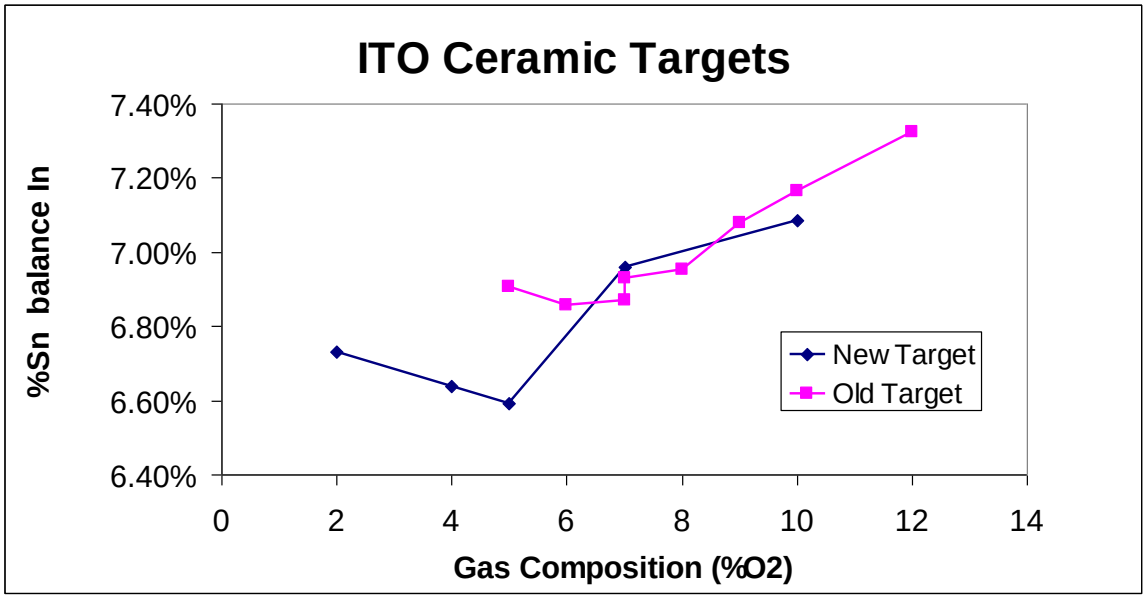

Figure 22. Comparison of target composition as a function of sputter gas composition for old and new targets.

The calculated coating thickness (Angstroms) to attain 10, 7.5 and 5 ohms per square as a function of temperature (°C) is shown in Figure 23. The curves for the sheet resistance were calculated from the resistivity data. Clearly, high post heating temperatures and thicker coatings result in the lowest sheet resistance. As in any process, trade offs will have to be made depending on the applications. If a high light transmittance is required, then post heating temperatures of 200°C will be necessary in any case. If lower transmittances can be tolerated, or it is not possible to heat the substrate to high temperatures, then a thick ITO coating is necessary. Substrate heating requires longer cycle time and adds complexity to the process, but coatings with the lower sheet resistance and high transmittance can be produced. There is also a savings on coating material costs, since a thinner coating is as effective as a thicker coating deposited at low or room temperatures.

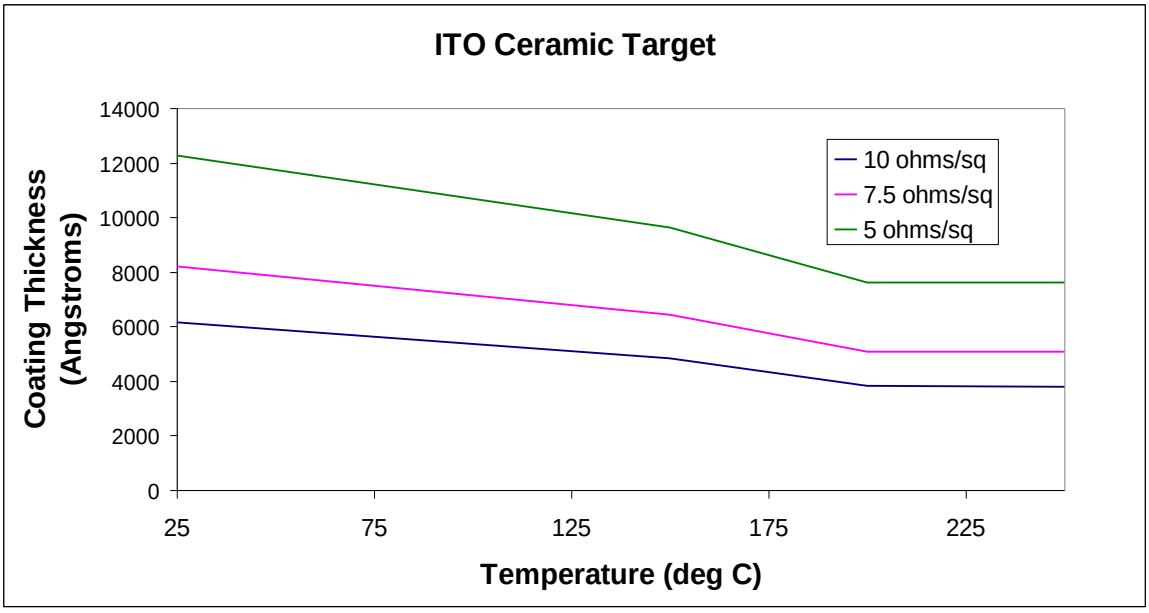

Figure 23. Calculated coating thickness required to achieve a given ITO sheet resistance as a function of post-deposition heat temperature.

The next step of this research was to scale up the process to produce uniform deposition on large substrates (12 inches square or greater) in preparation for Phase 2. The substrate used to develop the TCO coating was 2.3 mm thick clear float glass. In addition, several types of tinted and an ultra clear glass manufactured by PPG Industries were coated in anticipation of testing the effect of combinations of visible and ultraviolet light on the stability of the electrochromic polymers during Phase 2. Only a summary of the ITO coating development using these glasses will be reported here. The coatings were deposited from a ceramic ITO target with a composition of 5 percent indium by planar magnetron sputtering. The target was energized using an AE Pinnacle Plus power supply set to a constant power of 3.5 kW. The voltage and current of the target were 425 volts and 8.22 amps, respectively at this power setting. The coater was pumped down to a base pressure of less than 10^{-5} torr. During sputtering, the gas composition was fixed at 3 percent oxygen with a balance of argon, and the gas flow was maintained to keep a constant pressure of 1.8 millitorr. The substrate remained stationary above a resistance heater at a temperature of 550°F during deposition. The temperature of the substrate was monitored during deposition with a thermocouple attached to the bottom surface of the glass. The cathode target was conveyed over the substrate to deposit the coating as it scanned the length of the chamber. The transmittance was monitored *in situ* at a wavelength of 550 nm using a Dynoptics 580D optical monitor and recorded after each pass of the cathode over the substrate. The coating transmittance cycled through maxima (see Figure 24) indicating a multiple of a half wavelength optical thickness at 550 nm. Herein these multiples will be referred to as 1st, 2nd, 3rd and 4th reds. Each coated sample was run to an optical thickness of these four reds (see Table 4).

Physical thicknesses and sheet resistance (Rs) were measured after deposition, as well as transmittance, and reflectance in the ultraviolet, visible, near and far infrared. Sheet resistance was measured using an Alessi CPS-05 contact probe station and a Kiethley 2010 multimeter. The spectrophotometry measurements were made using a PerkinElmer Lambda 9 for wavelengths

between 300 and 2500 nm, and the far infrared measurements were made using a Mattson Galaxy 5030 Series FTIR for wavelengths from 5 to 40 micrometers. Hemispherical emissivity (E_h) was calculated using the emittance method outlined in ASTM E 1585-93 over the wavelength range from 5 to 40 micrometers. X-Ray fluorescence (XRF) was used to determine the composition and concentration of indium and tin in the coating and X-ray diffraction (XRD) was used to determine the crystalline phase of the coating. Direct measurements of thickness were made using a Tencor stylus profilometer. A linear least squares regression was used to develop an equation to calculate coating thickness using the indium concentration in the coating. Coating resistivity expressed in terms of μohm-cm was calculated in a similar manner using the relationship between the coating thickness and sheet resistance measurements.

The data for the ITO samples is listed in Table 4. Both the air and tin side of the float glass were coated. The half wave optical thickness or number of reds is shown with the corresponding percent transmittance, coating thickness in Angstroms, the amount of indium in the coating in micrograms per cm^2, sheet resistance in ohms per square and hemispherical emissivity.

Table 4. Properties of ITO Coated onto Clear Glass

Sample	Glass Surface	# of reds	% T at red	Coating Thickness (Å)	[In] ($\mu g/cm^2$)	R_s (ohms/sq)	E_h
57	Tin	1	89.3	1524	86.6	16	
58	Tin	2	87.7	2884	163.1	7.9	
59	Tin	3	85.5	4401	232.6	4.8	
60	Tin	4	82.5	5895	295.6	3.8	0.112
61	Air	1	89.1	1474	88.0	15.1	
62	Air	2	87.6	3119	172.1	7	
63	Air	3	85.4	4530	237.3	4.7	
56	Air	4	81.5	6056	298.9	3.4	0.107

Figure 24 shows the *in situ* optical transmittance of the ITO coating as a function of the number of passes of the cathode target over the substrate and coating thickness for sample 60. The peaks indicate the half wave optical thickness values where the transmission reaches a maximum value for the physical thickness. A refractive index of 1.84 is calculated using these data and is in agreement with data for coatings with high substrate temperatures.

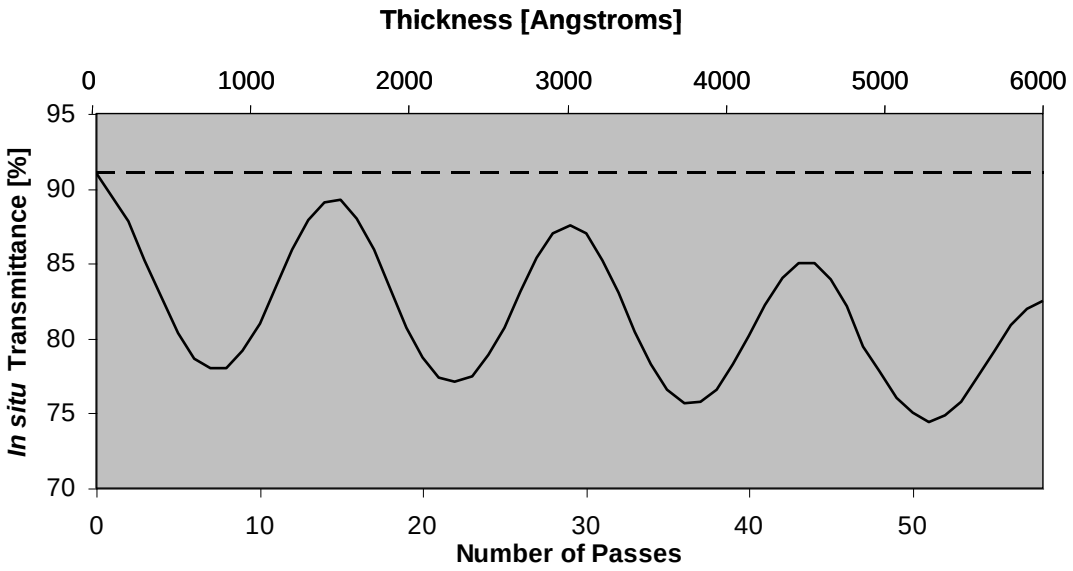

Figure 24. Transmittance curve for ITO coated glass, sample 60, as a function of the coating thickness and number of passes over the substrate coating.

Figure 25 shows the behavior of sheet resistance in ohms per square after deposition of each of the coatings listed in Table 4, as a function of inverse thickness in Angstroms^{-1}. A resistivity of 220 µohm-cm for the ITO coating was calculated using a least squares fit to the data of the inverse thickness versus sheet resistance as indicated by the straight line.

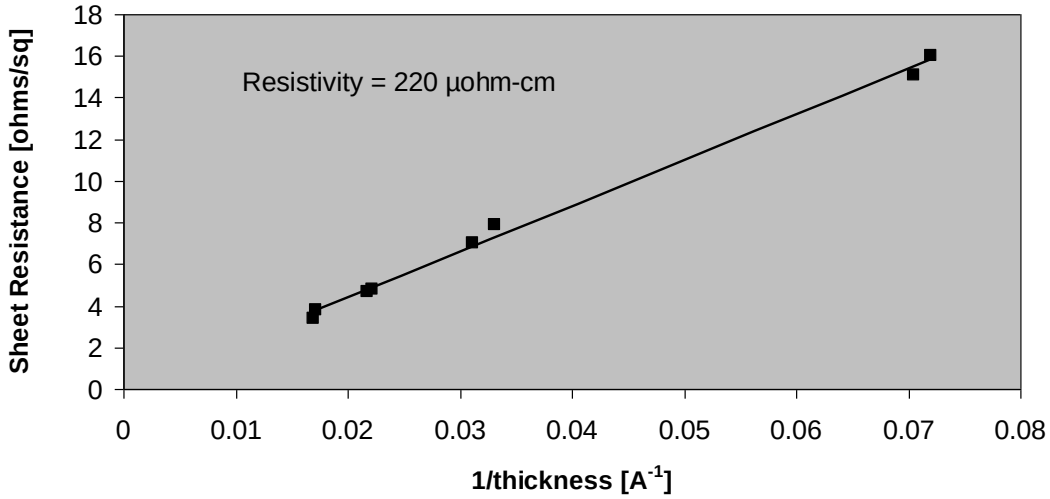

Figure 25. Sheet resistance as a function of 1/thickness for ITO coated glass.

The dependence of transmittance and reflectance as a function of wavelength over the range from 300 to 50000 nm (log scale) is shown for sample 60 in Figure 26. The reflectance spectrum indicates an onset of plasma or Drude edge at about 1350 nm in agreement with a coating in the

220 µohm-cm resistivity range. A hemispherical emissivity of 0.11 was calculated from the data in the wavelength range of 5 to 40 nm.

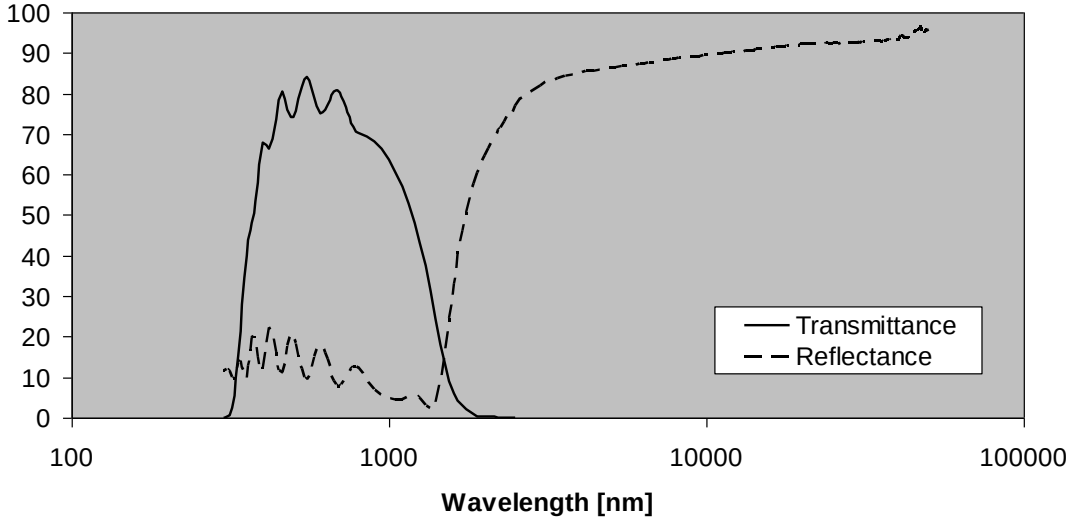

Figure 26. Optical data for ITO coated glass as a function of wavelength.

Figure 27 shows the XRD pattern of the ITO film. The peaks closely match the cubic, polycrystalline structure of ITO (PDF 00-006-0416).

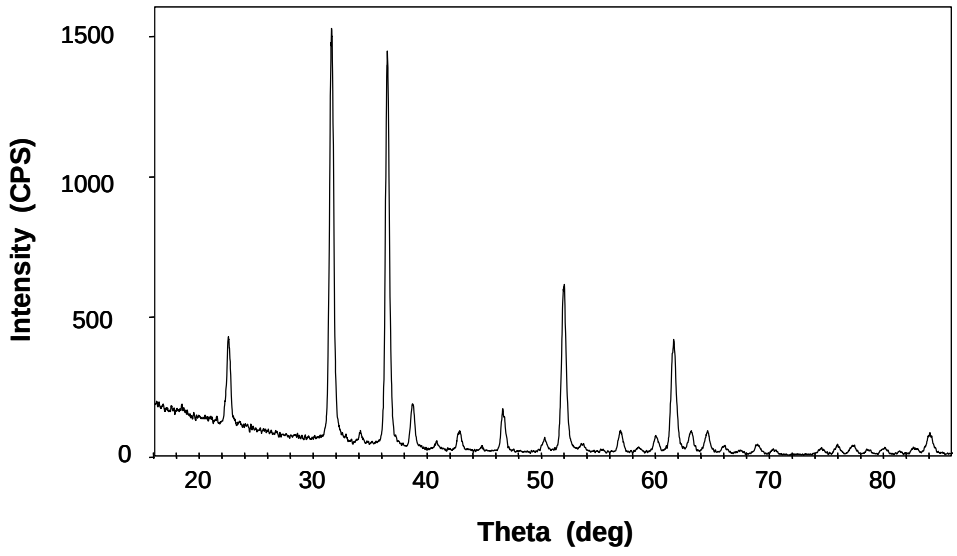

Figure 27. XRD pattern for the ITO coated glass film.

Finally, work was started on depositing the 2nd red ITO coating onto the air side of tinted and ultra clear glasses manufactured by PPG. This work (i.e., determination of transmittance and sheet resistance values, for Solex® and Solargreen® which are high iron containing infrared absorbing glasses, and Starphire® which is an ultraclear low iron glass) is being conducted in anticipation of proceeding to Phase 2. These glasses have different absorption characteristics in the UV and visible regions of the spectrum. The 2nd red transmittance for the different glasses as measured in the coater along with the thickness and sheet resistance are shown in Table 5.

Table 5. Properties of ITO Coated onto Various Glass Substrates

Sample	Substrate	Substrate Thickness (mm)	Transmittance	R_s (ohms/sq)
68	Solex	2.1	84.1	6.77
69	Starphire	2.3	88.4	6.97
70	Solargreen C5	2.0	82.1	7.03

For Phase 2, the optical properties of the ITO coating need to be determined and the coating parameters optimized for transmittance and sheet resistance for application within the electrochromic cell. The different glass types should be explored for their effect on limiting UV and their overall effect on shading coefficient. Pending the results of the stability of the coating when used in the electrochromic cell, additional layers will be added to the ITO coating stack to enhance the electrochromic cell's performance.

In addition to depositing ITO coatings, Phase 1 work also included examining a F:SnO_2 coating that was deposited in-house by the chemical vapor deposition process. The coating has a sheet resistance of 13 ohms per square. The primary driver in conducting this work was the cost savings that the F:SnO_2 coating would provide over the much more expensive ITO coated glass. The optical properties are similar when each of the TCO coating is incorporated into an electrochromic device as noted in Figure 28; however, additional work needs to be done to optimize the devices for the desired contrast range prior to conducting environmental testing experiments. The PTRs for the devices are also similar: 3.0 for the F:SnO_2 versus 3.2 for the ITO. The spectral differences are most likely due to the differences in the glass thicknesses. The glass is 1.0 mm thick for the ITO coated glass and 3.2 mm for the F:SnO_2 coated glass.

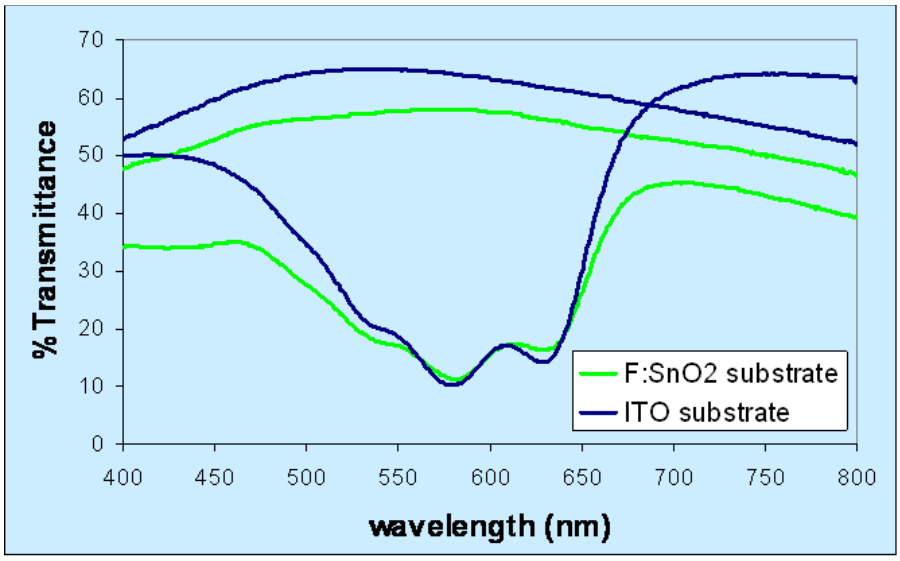

Figure 28. Spectral data for F:SnO_2 versus ITO. Stack sequence: glass/TCO/PANI/BMIM-BF_4 in PVDF membrane/PMAF-15/POT/TCO/ glass.

Task 4.0—Build and Evaluate 3"x 2" Devices

We continually modified and optimized the devices based on durability and energy performance results throughout Phase 1 of the project. The goal for Phase 1 was to satisfy the success criteria as outlined in the original contract for at least one device configuration with:

4.1. Aesthetically desirable bleached and darkened state color
4.2. Uniformity of color over a monolithic surface such that ΔE_{cmc} is less than 3 MacAdam units for any two points on the window
4.3. Coloration/decoloration times less than 2 minutes
4.4. Contrast degradation less than 5 percent over 50,000 coloration/decoloration cycles
4.5. Durability according to ASTM E2141 or NREL methods
4.6. Energy performance demonstrating reduction of solar heat load over that of traditional low-E technology
4.7. Commercial manufacturing cost defensibly estimated to be less than $100 per square foot

Subtask 4.1. Aesthetically desirable bleached and darkened state color

One of the advantages of using OSCPs is that the color can be tuned in with the selection of the polymer. Professor Reynolds at the University of Florida has done extensive research in this area developing polymers with a variety of colors in the bleached and colored states.[9,10] To achieve the maximum shading effect, we concentrated our efforts on targeting absorption in the darkened state at approximately 555 nm where the eye perception is the most sensitive. Color is a personal preference and passing this criterion will ultimately be the decision of the consumer. Generally speaking, neutral colors are more desirable in the marketplace; however it is believed that blue/dark blue will also be

[9] Welsh, D. M.; Kumar, A.; Meijer, E. W.; Reynolds, J. R. *Adv. Mater.* **1999,** *11*, 1379
[10] Thompson, B. C.; Schottland, P.; Zong, K.; Reynolds, J. R. *Chem. Mater*. **2000**, *12*, 1563-1571

an acceptable color for shading.

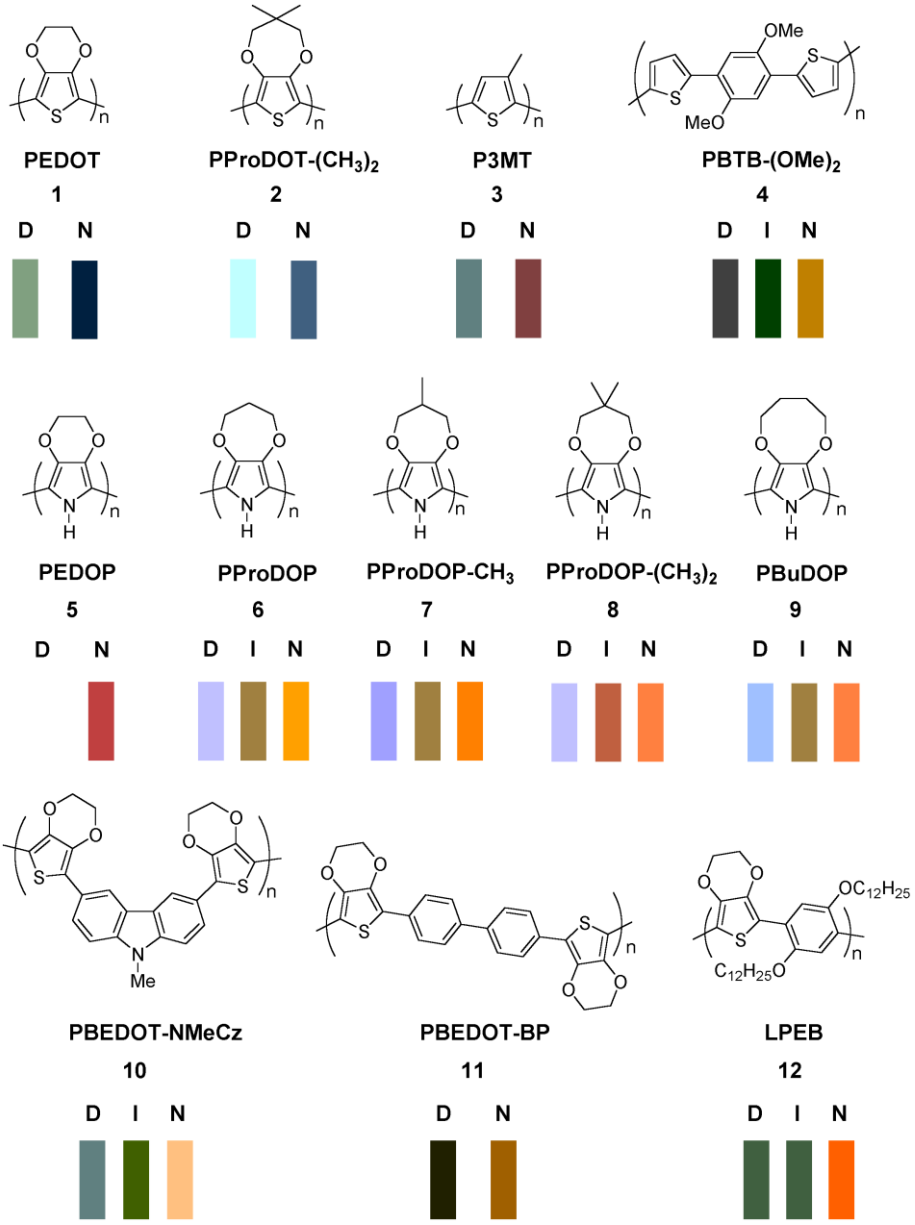

Figure 29. Various OSCP's with their colors in the doped, intermediate and neutral states represented.

The optimized device has a bleached state transmittance of 53.6 ± 2.5 percent and a dark state transmittance of 4.5 ± 1.3 percent. A photograph of each state is shown in Figure 30. The color coordinates for illuminant D65, 10^{o} observer are L* = 81.10, a* = -2.39 and b* = -1.73 in the bleached state and L* = 34.27, a* = 14.80 and b*= -44.33 in the colored/dark state.

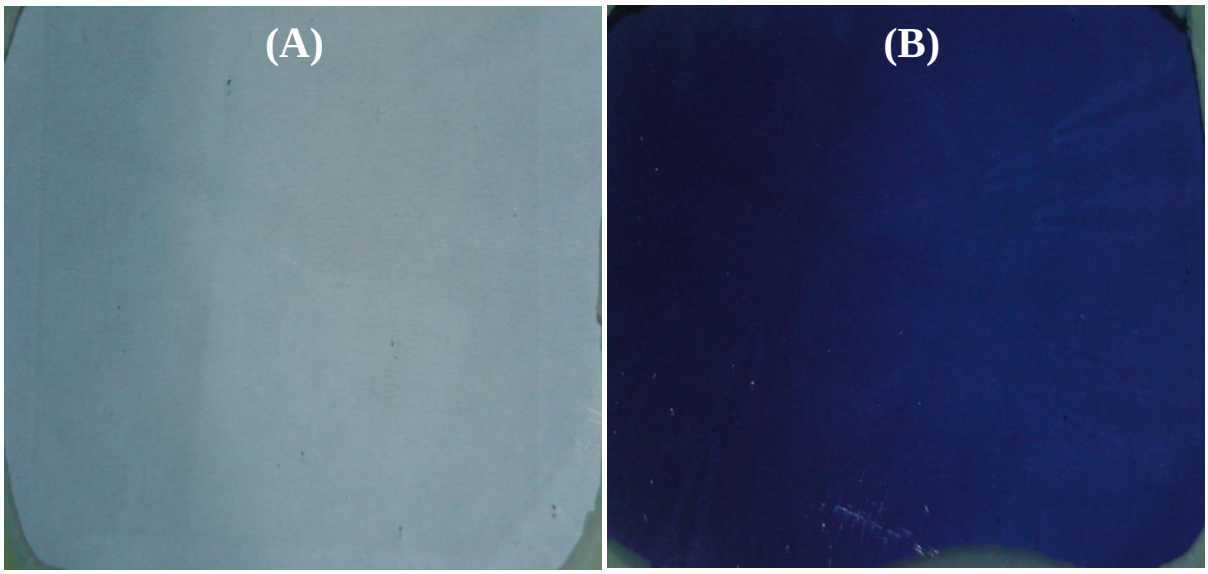

Figure 30. Photographs of an optimized electrochromic device in the (a) bleached state and (b) the colored/dark state. The percent transmittance of the bleached state is 53.6 ± 2.5 and the percent transmittance of the colored/dark state is 4.5 ± 1.3 at λ = 582 nm.

Subtask 4.2. Uniformity of color over a monolithic surface such that ΔE_{cmc} is less than 3 MacAdam units for any two points on the window

Uniformity is primarily linked to process conditions. For Phase 1, the current processing methods (i.e. spin coat) have been chosen for convenience, not uniformity. Uniformity will play a role when developing the deposition techniques for larger scale devices (i.e. Phases 2 and 3) and will be considered at that time.

Subtask 4.3. Coloration/decoloration times less than 2 minutes

Figure 31a shows a representative switching time for an early 2 inch by 3 inch electrochromic device. Note that this was one of the first devices that was made; therefore, the contrast is low; however, it is representative of the switching times observed for the optimized devices as well. The percent transmittance changes within seconds when voltage is applied whether going from the colored to the bleached state or from the bleached to the colored state. It has been observed that the devices do exhibit a decrease in switching time with UV exposure or elevated temperature.

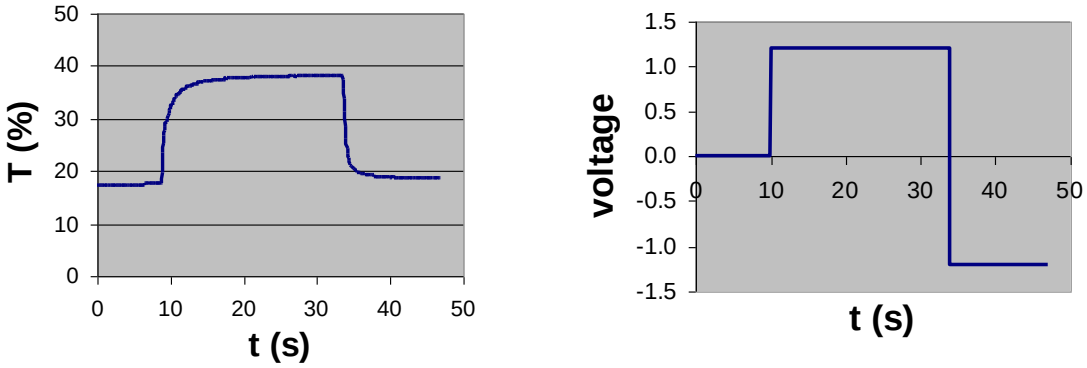

(a) (b)

Figure 31. (a) Representative switching time for an OSCP-IL electrochromic device. (b) Voltage versus time plot for curve 31a.

It has also been observed that the repeated application of a square voltage wavefunction as demonstrated in Figure 31b is detrimental to the function of the device. Figure 32 demonstrates how the transmittance in the colored state increases from 12 percent up to 50 percent after 40,000 cycles. The device is considered to have failed after a contrast of 40 percent is reached between 3000 and 4000 cycles. The problem with step voltage is that the controller used in the cycling study most likely spikes voltages greater than 2V which is detrimental to the system. ASTM 2141-06 suggests using a voltage ramp adequate for the system, i.e. 50 mV/s. All the cycling experiments in the remainder of the document were performed using a trapezoidal voltage rather than a step voltage.

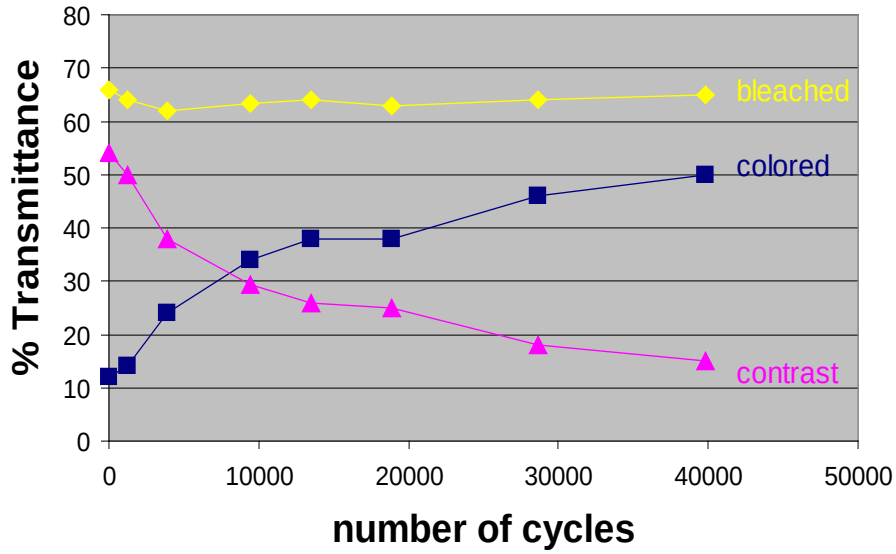

Figure 32. Continuous cycling of a device containing POT-PMAF-15/PANI with a square voltage ramp.

Subtask 4.4. Contrast degradation less than 5 percent over 50,000 coloration/ decoloration cycles

Samples exposed to ambient temperatures and low level fluorescent overhead lighting during the day were continually cycled at a rate of 50 mV/sec from -1.4 to +1.4V. Periodically, spectral data was collected with the sample held at either -1.5 or +1.5V to determine the bleached state and dark state transmittance. Data was collected either after the bleached or dark state was stabilized or within 30 minutes of applying the charge (as recommended in ASTM 2141-06). Figure 33 shows the transmittance data as a function of wavelength over time.

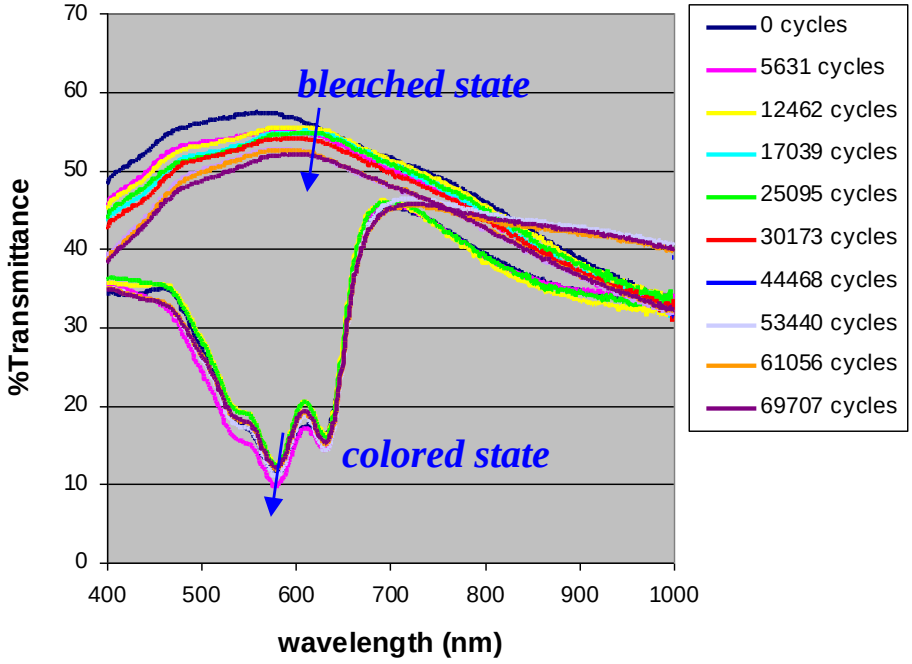

Figure 33. Spectral data for an optimized device as a function of number of cycles with ambient heat and no solar exposure. Cycle rate is 50 mV/sec. Cycle range is -1.4V to +1.4V.

The goal was to maintain the bleached state transmittance above 50 percent and the contrast above 40 percent after 50,000 cycles with less than 5 percent change. After 53,440 cycles, the sample passed with approximately 4 percent change (see Figure 34Figure 34). The sample was cycled for an additional 16,267 cycles and only 5.5 percent change was observed. This test is considered to be complete with passing results.

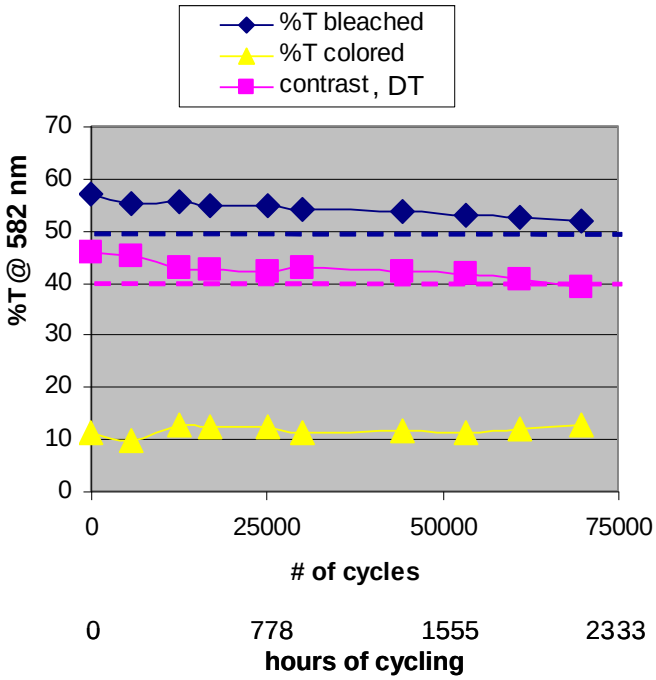

Figure 34. Durability performance with continuous cycling at 50 mV/sec from -1.4 to +1.4V, ambient heat and no solar exposure.

Subtask 4.5. Durability according to ASTM E2141 or NREL methods.

When durability performance testing was initiated, sealant failure dominated the device failure. With exposure to the accelerated weathering conditions, the seal did not survive and the electrolyte leaked out of the cell causing the electrochromic polymers to be unable to undergo redox reactions.

To examine the sealant failure, the conductive polymer films were removed from the device and a cell comprised of just the ionic liquid soaked membrane was evaluated between two pieces of clear glass with various sealants and sealant configurations. During this testing, we discovered that most of the membranes within the samples became yellow. It is believed that the yellowing is due to UV degradation of uncured sealant that has migrated into the membrane. The membrane concentrates the components and appears yellow when the material degrades with UV exposure. Improvements were made by varying the chemistry of the sealant to eliminate this effect. The results are shown in Figure 35 after 300 hours of exposure at 0.52 W/m^2 (xenon arc) and 85^oC. The device depicted in Figure 35A shows the worst yellowing and Figure 35F shows the least yellowing. For the remainder of the testing covered within this report, a non-interacting sealant was selected that behaves similarly to the sample shown in Figure 35F.

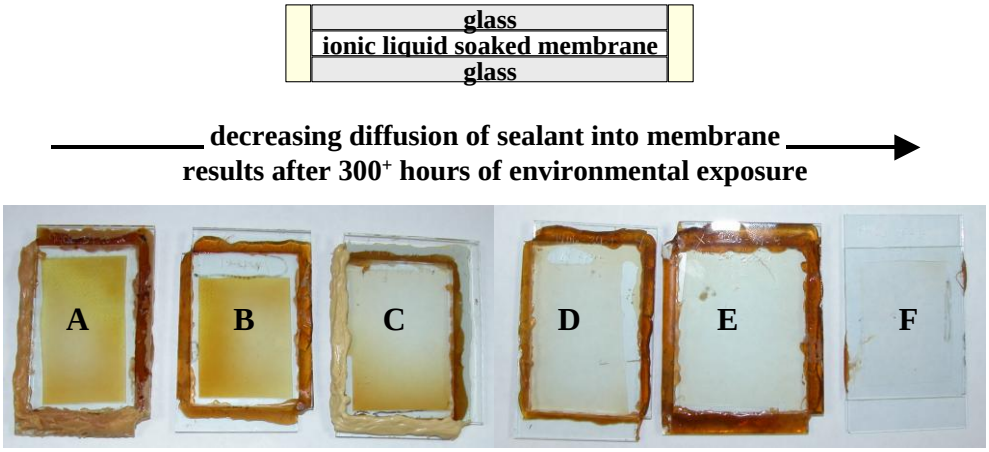

Figure 35. Electrochromic cells demonstrating the effect of sealant configuration on the yellowing of membranes soaked in ionic liquid.

For screening device durability, NREL recommended the following testing scenarios based on ASTM 2141-06 (Standard Test Methods for Assessing the Durability of Absorptive Electrochromic Coatings on Sealed Insulating Glass Units). Durability testing has been initiated for all of the testing conditions with the configuration and stack sequence depicted in Figure 2. Results for each condition are given below.

Table 6. Experimental Parameters

CONDITION	HEAT (85°C)	SOLAR (0.52 W/m^2)	CONTINUOUS CYCLING*
1	no	no	no
2	no	no	**YES**
3	**YES**	no	no
4	**YES**	**YES**	no
5	**YES**	no	**YES**
6	**YES**	**YES**	**YES**

**Cycling rate and voltage input are device dependent. For our testing the rate was set at 30 mV/sec and the range was from -1.5V to +1.5V.*

A summary of the results for each condition is given in Table 7. Overall, tremendous strides were made to increase the durability of the electrochromic cells and 4 of the 6 testing conditions outlined in Table 6 produced passing results; however, when cycling was introduced as a variable and heat was present, failures resulted. In a window application, the electrochromic polymers will be exposed to elevated temperatures. This combination appears to be detrimental to the degradation of the redox reactions which control the electrochromism of the device. Specific details of the work done for each condition are given in the remainder of this section.

Table 7. Results Summary for Durability Testing of Optimized Electrochromic Devices.

CONDITION	HEAT 85°C	SOLAR 0.52 W/m²	CYCLING -1.5 to +1.5V	EXP TIME (hrs)	# CYCLES	%$T_{bleached}$ @ 582 nm	%T_{dark} @ 582 nm	CONTRAST (ΔT)	STATUS
1	NO	NO	NO	5018	na	53.4 ± 1.1	7.1 ± 1.9	46.3	PASSED
2	NO	NO	YES	na	68,815	50.0	6.6	43.4	PASSED
3	YES	NO	NO	5080	na	48.0	5.2	42.8	PASSED
4	YES	YES	NO	1059	na	49.3	5.9	43.4	testing stopped so that equipment could be used to perform 65°C evaluations
	YES 65°C	YES	NO	4274	na	51.8	5.8	46.0	in progress, PASSING
	YES 45°C	YES 0.83 W/m²	NO	5000	na	51.5	13.1	38.4	PASSED
5	YES	NO	YES	302	5,436	47.9	5.8	38.1	FAILED between 160 and 302 hrs
	YES 65°C	NO	YES	773	13,914	44.9	4.1	40.8	FAILED
6	YES	YES	YES	180	3,240	44.5	4.8	39.7	FAILED
	YES 65°C	YES	YES -1.2 to +1.2V	455	10,238	42.4	5.4	37.0	FAILED

Condition 1: Control with no heat, no solar and no continuous cycling. Samples were maintained on the bench top in the laboratory. They experienced ambient temperatures and were exposed to low level fluorescent overhead lighting during the day. Periodically, the devices were cycled five times from -1.5 to +1.5V, then spectral data was collected with each sample held at either -1.5 or +1.5V to determine the bleached state and dark state transmittance. Data was collected either after the bleached or dark state was stabilized or within 30 minutes of applying the charge (as recommended in ASTM 2141-06). Figure 36 shows the transmittance data as a function of wavelength over time.

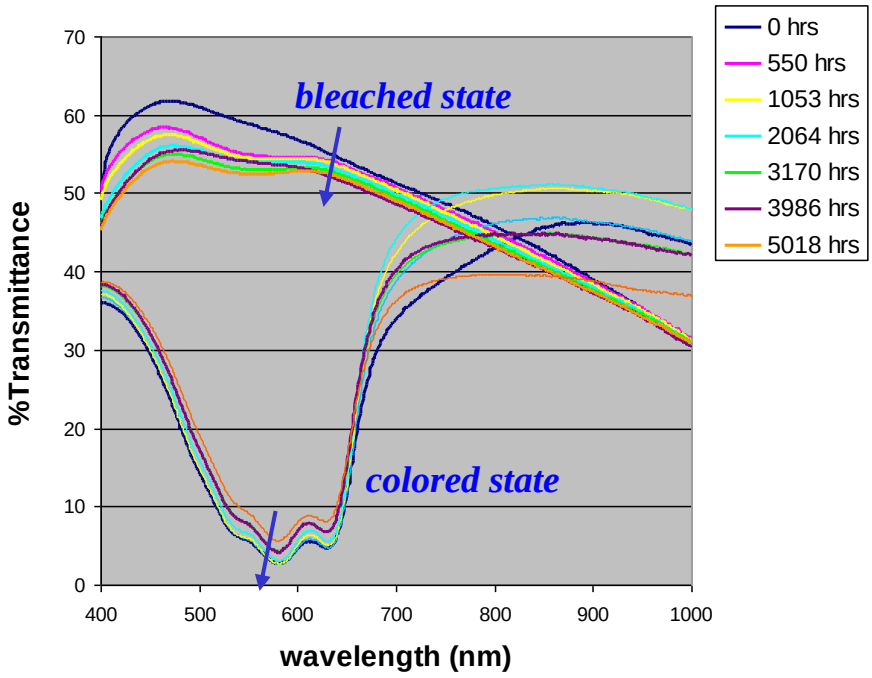

Figure 36. Spectral data for an optimized electrochromic device as a function of time. The device experienced ambient heat, no solar exposure, no continuous cycling.

Durability and device stability was determined by plotting the percent transmittance at 582 nm as a function of exposure time (see Figure 37). Samples were considered to pass if the bleached state was maintained above 50 percent transmittance and the contrast above 40 percent transmittance. After 5018 hours, the sample passed with less than 2 percent change for either the bleached state transmittance or the contrast.

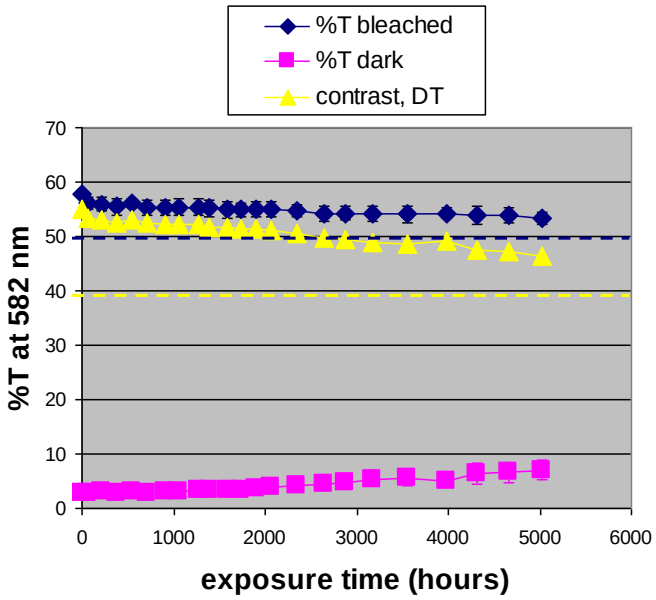

Figure 37. Durability performance for devices exposed to ambient heat with no solar exposure and no continuous cycling.

Condition 2: Continuous cycling with ambient heat and no solar exposure. See Subtask 4.4 for passing results.

Condition 3: Elevated temperature with no solar exposure and no cycling. A total of 8 samples were placed in an oven at 85^{o}C. These samples experienced no cycling or solar exposure while in the oven. Periodically, they were removed from the oven and cycled five times from -1.5 to +1.5V, then spectral data was collected with the devices held at either -1.5 or +1.5V to determine the bleached state and dark state transmittance. Data was collected either after the bleached or dark state was stabilized or within 30 minutes of applying the charge (as recommended ASTM 2141-06). Figure 38 shows the transmittance data as a function of wavelength over time for two of the samples. Sample 9406-47-11 of Figure 38A is an older sample which failed after approximately 100 hours of exposure. Sample 1016-cmb-4 (Figure 38B) is a newer sample with a modified device construction. A dramatic improvement is observed between the two plots for the bleached state data.

Figure 39 shows the improvement in durability when modifications were made to the device construction. Durability and device stability is determined by plotting the percent transmittance at 582 nm as a function of exposure time. Passing criteria is to maintain the bleached state above 50 percent transmittance and the contrast above 40 percent transmittance for 5000 hours.

Earlier samples such as 9406-47-11 fail the 50 percent transmittance requirement within 50 hours of testing, while the newest sample, 1016-cmb-4, marginally passed the 50 percent transmittance requirement after 5000 hours of exposure (Figure 40). After 5000 hours of exposure, the bleached state transmittance is just below the 50 percent

requirement and the contrast passes at greater than 40 percent. It is noteworthy that we were able to extend the durability considerably to achieve passing results with improvements in device construction and sealant selection.

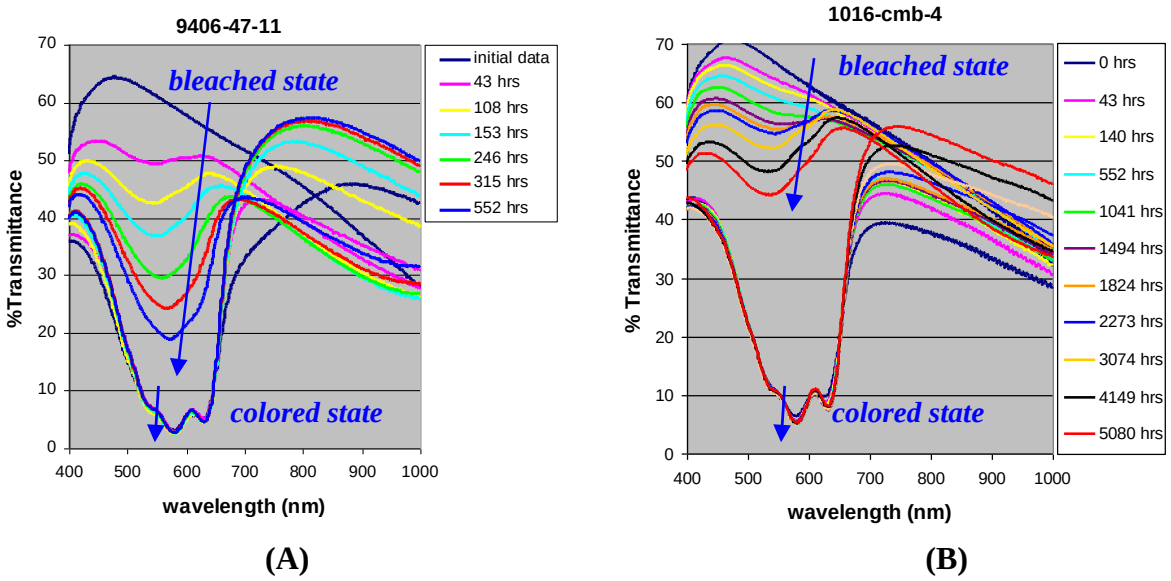

(A) **(B)**

Figure 38. Spectral data for 2 optimized devices as a function exposure time: (A) older sample and (B) newer sample with improved sealant and device construction. Samples exposed to 85°C with no solar exposure and no continuous cycling.

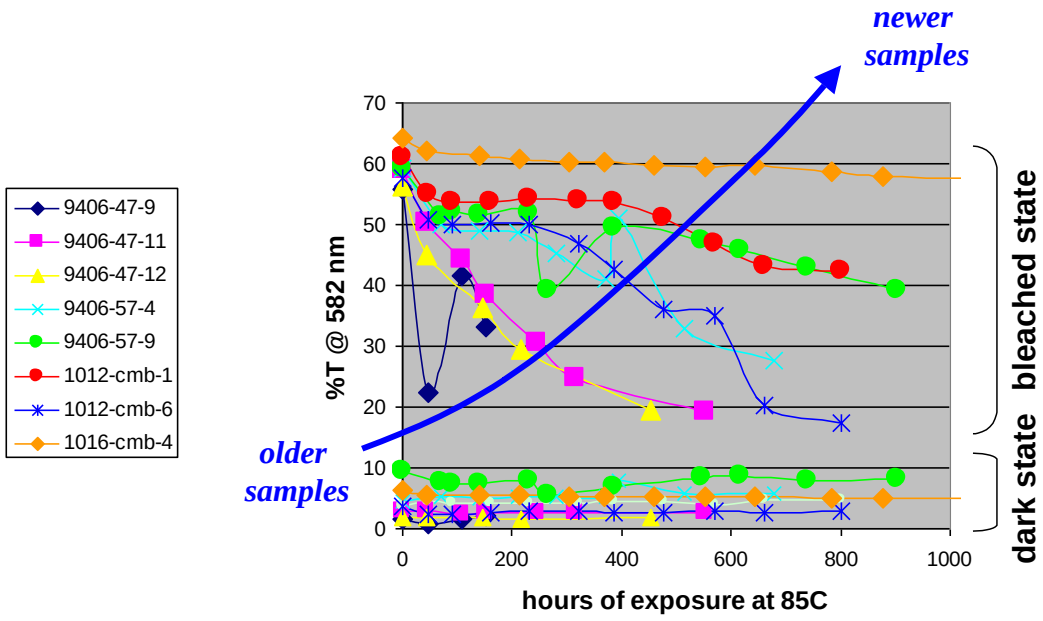

Figure 39. Improvements in device durability with heat exposure at 85°C with progressive modifications to sealant and device construction. Devices experienced no continuous cycling and no solar exposure.

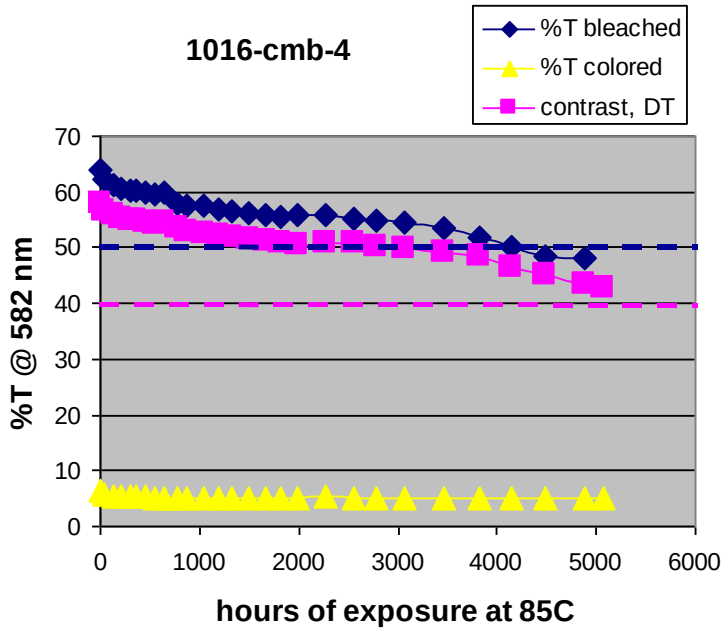

Figure 40. Durability performance for an optimized electrochromic device with heat exposure at 85°C. The device experienced no continuous cycling and no solar exposure.

Condition 4: Elevated temperature and solar exposure with no cycling. A total of 7 samples were exposed to solar irradiation from a xenon arc source in a QSUN® environmental chamber at 0.52 W/m^2 and 85°C with no continuous cycling. Periodically, each of the samples was removed and cycled five times from -1.5 to +1.5V, then spectral data was collected with the device held at either -1.5 or +1.5V to determine the bleached state and dark state transmittance. Data was collected either after the bleached or dark state was stabilized or within 30 minutes of applying the charge (as recommended in ASTM 2141-06). Figure 41 demonstrates the dramatic improvement in durability by modifying the device construction and sealant selection. Durability and device stability is determined by plotting the percent transmittance at 582 nm as a function of exposure time. Passing criteria is to maintain the bleached state above 50 percent transmittance and the contrast above 40 percent transmittance for 5000 hours.

Older samples such as 9406-47-3 failed within 50 hours of testing, while the newest sample 9406-57-5 is passing the 50 percent transmittance requirement after 1,059 hours of exposure. Data for sample 9406-57-5 is also shown in Figure 42. The bleached state transmittance is holding steady at 50 percent transmittance and the contrast is greater than 40 percent transmittance.

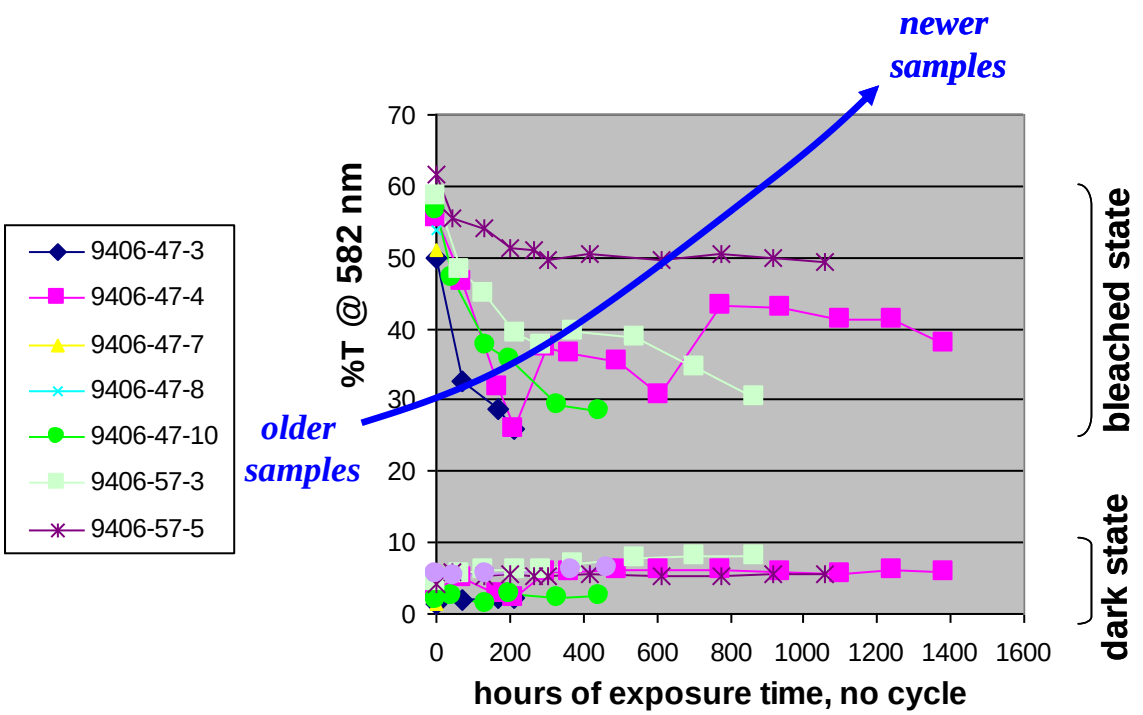

Figure 41. Improvements in electrochromic device durability with solar exposure at 0.52 W/m^2, heat exposure at 85^{o}C and no continuous cycling. Progressive improvements were made regarding sealant and device construction.

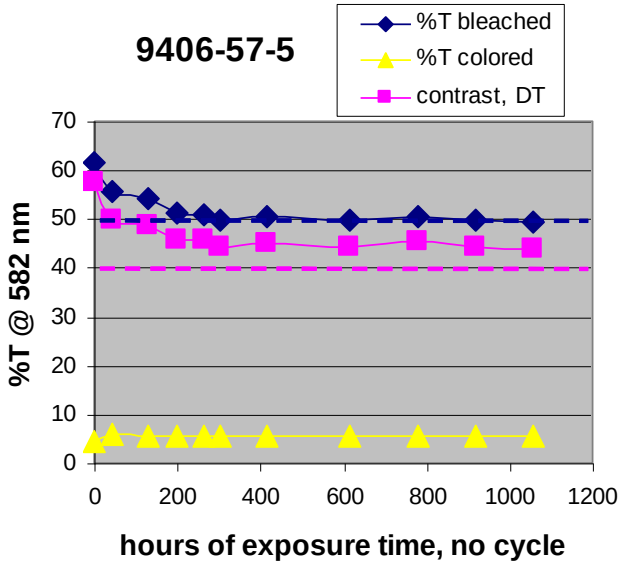

Figure 42. Durability performance for an electrochromic device in a QSUN® environmental exposure chamber with solar exposure (xenon arc) at 0.52 W/m^2, heat exposure at 85^{o}C and no continuous cycling.

Early in the project, durability testing was initiated in a QUV® chamber at 45°C. This testing unit uses UVA-340 bulbs that mimic the ultraviolet portion of the solar spectrum. The primary difference in the QUV and the QSUN testing is that the QUV does not include the infrared portion of the solar spectrum and the temperature in the QUV was 40 degrees lower than the temperature in the QSUN. In the QUV, the irradiation level was set at 0.83 W/m^2. The sample in this unit was monitored for 5000 hours of testing over the course of approximately one year. This sample has the same stack configuration as noted in Figure 2; however, the layers were not optimized for contrast and the sealant and device construction had not been improved upon. It is notable that this device maintained contrast above 40 percent transmittance between 4300 and 4900 hours. The bleached state transmittance also stayed above 50 percent during a majority of the testing (see Figure 43).

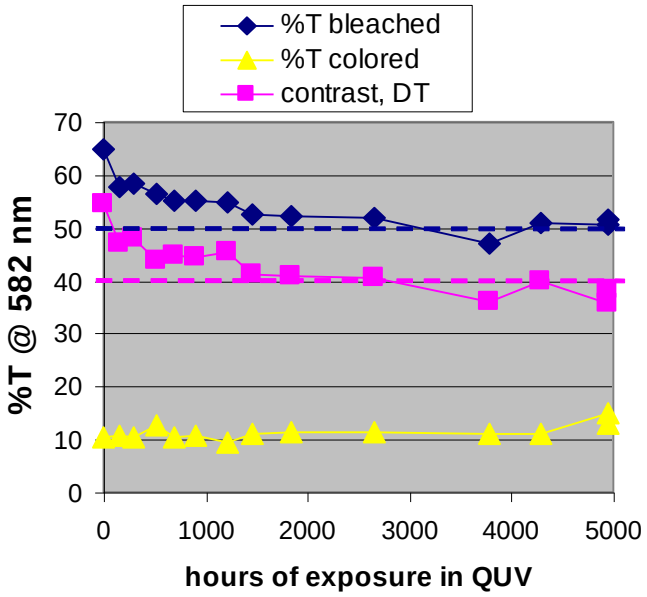

Figure 43. Durability performance for an electrochromic device in a QUV® environmental exposure chamber with ultraviolet exposure (UVA-340) at 0.83 W/m^2, heat exposure at 45°C and no continuous cycling.

Upon comparing the 85 and 45°C results, we wanted to have a better understanding of the temperature that the insulated glass unit (IGU) would be exposed to in the field so thermal simulations were performed with the electrochromic device incorporated into an IGU, to see how realistic the 85°C recommendation was that was given in the ASTM 2141-06 method for our proposed IGU. A schematic of which is given in Figure 44. The data was generated using LBNL's WINDOW 5.2[11] software (v5.2.17) with NFRC 100-2001 summer conditions: inside air = 24°C, outside air = 32°C, direct solar radiation = 248.2 Btu/hr-ft^2 with an outside wind speed = 6.2 mph. The results for the temperatures at the center of the glass for a 1 meter by 1 meter unit with ½ inch gap filled with 90 percent argon and 10 percent air are given in Table 8.

[11] http://windows.lbl.gov/software/window/window.html

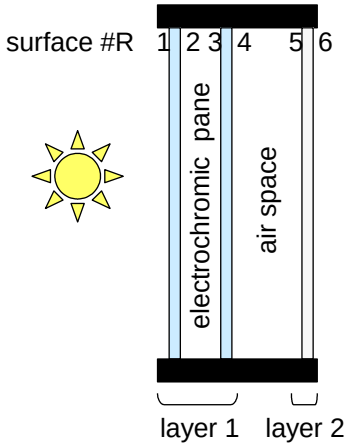

Figure 44. Insulated Glass Unit Configuration for Thermal Simulations

Table 8. Predicted surface temperatures of various IGU configurations with and without low-E coatings included					
Configuration		**Temperature ^{o}C**			
layer 1	**layer 2**	**layer 1**		**layer 2**	
		outside	**inside**	**outside**	**inside**
EC Pane BLEACHED	clear	48.9	49.8	37.2	36.9
EC Pane TINTED	clear	52.9	54.0	39.2	38.8
EC Pane BLEACHED	SB60 (R5)	52.9	54.2	34.7	34.5
EC Pane TINTED	SB60 (R5)	57.7	59.2	33.8	33.7
EC Pane BLEACHED	SB70XL (R5)	53.8	55.2	35.7	35.5
EC Pane TINTED	SB70XL (R5)	58.5	60.2	33.8	33.6
EC Pane BLEACHED with SB60 (R4)	clear	54.4	55.8	31.2	31.0
EC Pane TINTED with SB60 (R4)	clear	58.5	60.1	31.8	31.7
EC Pane BLEACHED with SB70XL (R4)	clear	55.9	57.4	30.8	30.6
EC Pane TINTED with SB70XL (R4)	clear	59.5	61.2	31.3	31.2

Note: EC pane is an optimized electrochromic pane, SB60 is Solarban®60 low-E coated glass and SB70XLis Solarban® 70XL low-E coated glass, both of which are products of PPG Industries, Inc.

The simulations demonstrate that the highest temperature that the electrochromic layer would experience under these conditions is 61.2^{o}C (highlighted orange in Table 8). This temperature is much less than the 85^{o}C temperature recommended in the ASTM 2141-06 test. It is understood that testing at elevated temperatures is only meant to accelerate the degradation process; however, the results generated thus far have raised concerns as to

whether this may lead to degradation paths that might not be experienced at lower temperatures. At this stage in the development of this technology, it may be more appropriate to study the systems at lower temperatures. When samples were exposed at 0.52 W/m^2 in the QSUN at 65^{o}C rather than 85^{o}C, they have maintained passing levels for bleached state transmittance and contrast after 4274 hours of testing and are anticipated to still be passing after 5000 hours of testing at 65^{o}C (see Figure 45). These results are significant in that the devices essentially pass the testing at 65^{o}C and the simulations indicate that the 65^{o}C temperature is representative of the real-life field exposure temperature.

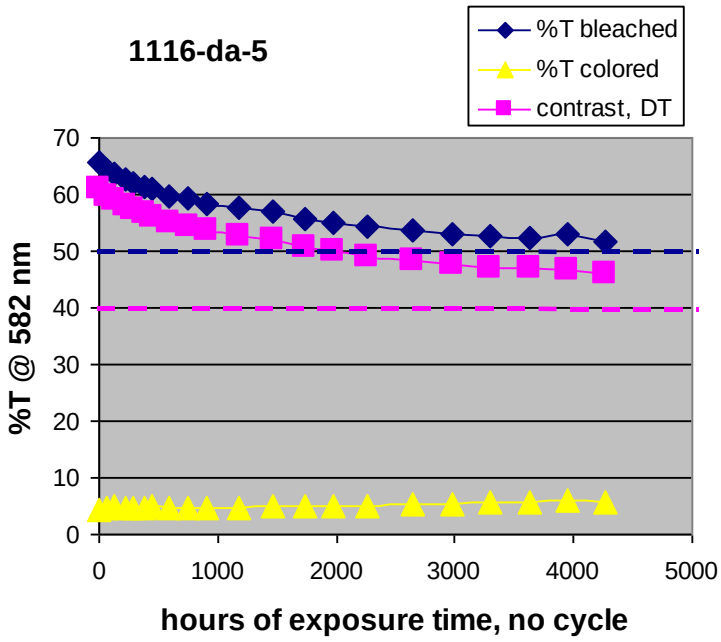

Figure 45. Durability performance for an electrochromic device in a QSUN® environmental exposure chamber with solar exposure (xenon arc) at 0.52 W/m^2, heat exposure at 65^{o}C and no continuous cycling.

Condition 5: Elevated temperature with cycling and no solar exposure. A sample with the most improved device construction was heated in an oven at 85^{o}C with continuous cycling from -1.5 to +1.5V at a rate of 30 mV/sec. Periodically, the sample was removed from the heat and cycled five times from -1.5 to +1.5V, then spectral data was collected with the device held at either -1.5 or +1.5V to determine the bleached state and dark state transmittance. Data was collected either after the bleached or dark state was stabilized or within 30 minutes of applying the charge (as recommended ASTM 2141-06). At 85^{o}C, the sample fails in less than 200 hours of exposure. A duplicate sample showed the same result. When another sample set was cycled over the same range and rate at 65^{o}C, the durability was increased to approximately 500 hours (see Figure 46). It is noteworthy that the durability was increased; however, with the improved device construction and the

lower temperature, the 5000 hour goal is unobtainable. It seems that the cycling coupled with the elevated temperature is detrimental to the switching of the electrochromic cell.

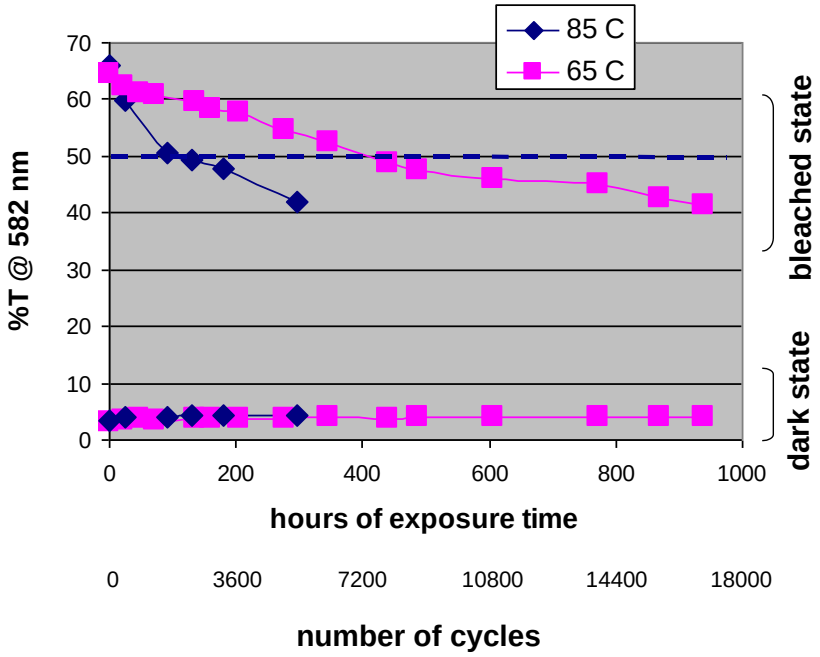

Figure 46. Durability performance for an optimized electrochromic device with heat exposure at 85 and 65°C. The devices experienced continuous cycling from -1.5V to +1.5V at a rate of 30 mV/sec with no solar exposure.

Condition 6: Elevated temperature with cycling and solar exposure. A total of 7 samples were exposed to solar irradiation from a xenon arc source in a QSUN® environmental chamber at 0.52 W/m^2 and 85°C with continuous cycling from -1.5 to +1.5V at a rate of 30 mV/sec. This condition looks at all of the variables (solar, heat and cycling) and is considered to be the harshest of the durability tests performed. Periodically, each of the samples was removed and cycled five times from -1.5 to +1.5V, then spectral data was collected with the device held at either -1.5 or +1.5V to determine the bleached state and dark state transmittance. Data was collected either after the bleached or dark state was stabilized or within 30 minutes of applying the charge (as recommended in ASTM 2141-06).

Figure 47 shows the data generated for the 7 samples. Only a marginal improvement is noted with the progressive modifications of the device construction and the best devices fail the 50 percent transmittance requirement within 200 hours of exposure.

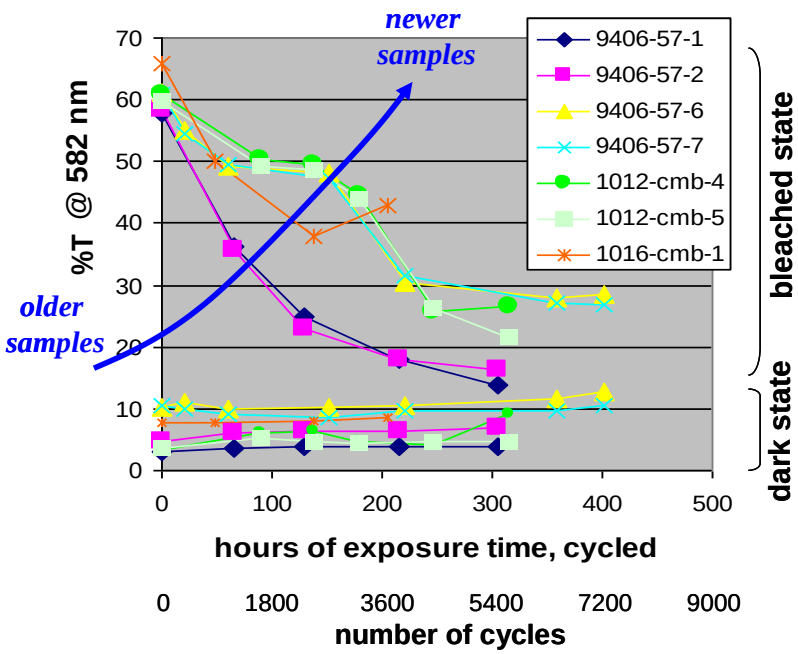

Figure 47. Improvements in durability with solar exposure at 0.52 W/m^2, heat exposure at 85^{o}C and continuous cycling from -1.5 to +1.5 V at a rate of 30 mV/sec. Progressive improvements were made regarding sealant and device construction.

In an attempt to improve the longevity of the electrochromic devices, the testing temperature was decreased to 65^{o}C which more adequately represents a real-life exposure and the cycling range was decreased to -1.2 to +1.2V. The results are given in Figure 48 which also includes data for devices exposed at 85^{o}C with a cycling range of -1.5 to +1.5V for comparison. By modifying the testing conditions, the rate of degradation was much slower but still did not approach the 5000 hour goal.

At this point, further improvements in device construction for this device configuration are not anticipated to result in a system that will survive under this testing for 5000 hours.

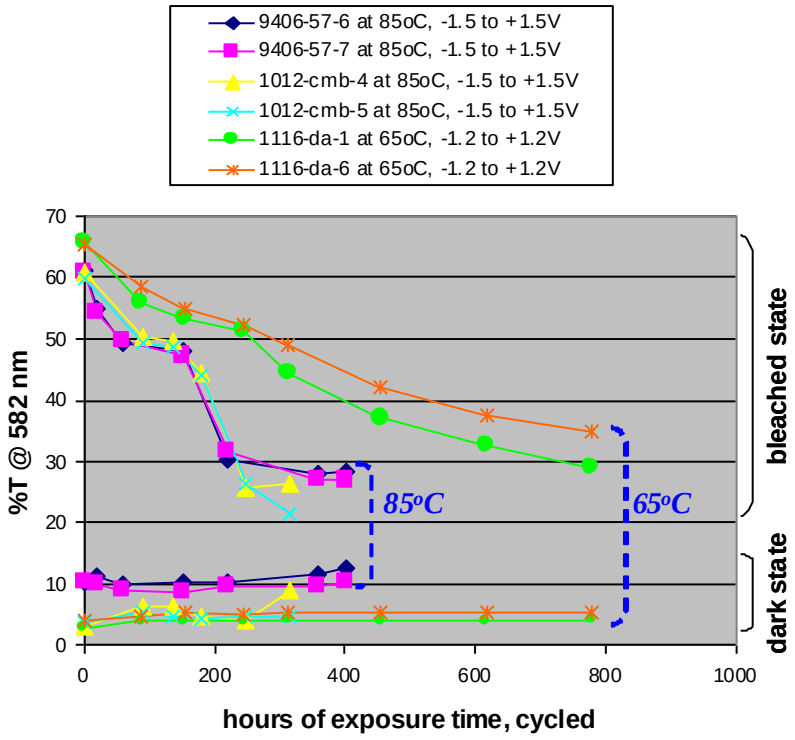

Figure 48. Electrochromic device durability comparison at 85°C and 65°C with solar exposure at 0.52 W/m^2. Cycling ranges from -1.5 to +1.5V and -1.2 to +1.2V, respectively.

Subtask 4.6. Energy performance demonstrating reduction of solar heat load over that of traditional low-E technology

The energy performance of the optimized electrochromic devices was gauged based on modeling simulations using LBNL's Windows 5.2[12] software (v5.2.17) for IGUs. A schematic representing the IGU and the various surfaces is given in Figure 44. For these simulations low-E coatings were also included on various surfaces within the IGU to evaluate their effect on the overall energy performance when coupled to the electrochromic device within the IGU. The U-value, solar heat gain coefficient (SHGC) and the light to solar gain ratio (LSG) were computed using NFRC 100-2001 summer conditions: inside air = 24°C, outside air = 32°C, direct solar radiation = 248.2 Btu/hr-ft^2 with an outside wind speed = 6.2 mph. Results are for the center of the glass of a 1 meter by 1 meter unit with a ½ inch gap filled with 90 percent argon and 10 percent air. All of the results are given in Table 9.

[12] http://windows.lbl.gov/software/window/window.html

Table 9. Predicted energy parameters of various electrochromic IGU configurations with and without low-E coatings included.					
layer 1	**layer 2**	**U-value**	**Tvis**	**SHGC**	**LSG***
clear	SB60 (R5)	0.220	72.2%	0.465	1.55
EC Pane BLEACHED	clear	0.478	50.0%	0.402	1.64
EC Pane TINTED	clear	0.478	7.5%	0.305	
EC Pane BLEACHED	SB60 (R5)	0.219	44.4%	0.290	2.70
EC Pane TINTED	SB60 (R5)	0.219	6.6%	0.165	
SB60 (R4)	clear	0.220	72.2%	0.385	1.88
EC Pane BLEACHED with SB60 (R4)	clear	0.219	45.2%	0.255	3.15
EC Pane TINTED with SB60 (R4)	clear	0.219	6.8%	0.144	
clear	SB70XL (R5)	0.210	64.1%	0.377	1.70
EC Pane BLEACHED	SB70XL (R5)	0.209	39.4%	0.248	3.07
EC Pane TINTED	SB70XL (R5)	0.209	5.8%	0.129	
SB70XL (R4)	clear	0.210	64.1%	0.272	2.36
EC Pane BLEACHED with SB70XL (R4)	clear	0.209	40.2%	0.197	3.92
EC Pane TINTED with SB70XL (R4)	clear	0.209	5.9%	0.103	

**LSG is Light to Solar Gain or Tvis/SHGC. For an EC, it is Tvis (bleached) / SHGC (tinted). EC pane is an optimized electrochromic pane, SB60 is Solarban®60 low-E coated glass and SB70XLis Solarban® 70XL low-E coated glass, both of which are products of PPG Industries.*

When the electrochromic layer is incorporated into an IGU with clear glass in the layer 2 position, the U-value is somewhat higher than that of an IGU containing only a low-E coating (0.478 versus approximately 0.21). However, the SHGC is comparable (0.305 dark state and 0.402 bleached state) to that of a typical IGU comprised of Solarban® 60 on R4 (0.385). The addition of the low-E coatings to the electrochromic device construction reduced the U-value from 0.478 to approximately 0.21. However, in each case, the Tvis was also reduced to values lower than 50 percent when the low-E coatings were coupled with the electrochromic technology. The system would have to be optimized further to maintain Tvis above 50 percent for the IGU when the low-E coatings are incorporated into the IGU. By adding low-E coatings to the R5 surface, SHGCs ranging from 0.290 to 0.165 for SB60 and 0.248 to 0.129 for SB70XL were achieved. The values could be decreased further if the low-E coating were placed on R4: 0.255 to 0.144 for SB60 and 0.197 to 0.103 for SB70XL. There are similar trends in the LSG

values. Coupling a low-E coating with the electrochromic devices reduces the overall SHGC.

To estimate the national total energy savings for the electrochromic technology, the energy savings will be compared to that of a typical double-silver low-E coated window. Next, the national energy consumption for end-use category is determined according to Table A.1 of the Announcement. The total energy used for cooling to counter solar transmission through windows is 0.785 quads and the energy penalty during the heating season is 0.712 quads. Finally the potential market penetration for the electrochromic window is estimated. Initial costs for electrochromic windows are estimated to be $50-$100 per square foot, ultimately falling to around $10 per square foot as market share increases.[13] Low-E windows currently available cost $6-$7 per square foot. This cost difference will limit market penetration. The payback period for electrochromic windows is estimated to be 1 to 3 years,[13] which will also limit market penetration. Low-E market penetration was just 35% after 15 years on the market. It is possible that the additional features of electrochromic windows, plus the fact that the consumer can "see" the difference with electrochromic windows, could improve the market penetration and shorten the time to achieve that penetration. Considering all of these factors, the potential market penetration is estimated to be 20%. As a result, the net energy savings is calculated as follows:

(1) relative net energy savings over that of a typical double-silver low-E coated window = potential cooling energy savings – potential energy penalty during the heating season

*(2) potential cooling energy savings = 0.785 quads * (SHGC for typical double-silver low-E coated IGU – SHGC of the electrochromic IGU in the tinted state) * 0.2*

where 0.785 quads is the total energy used for cooling to counter solar transmission through a window
and 0.20 = estimated market penetration

*(3) potential heating penalty = 0.712 quads * (SHGC for typical double-silver low-E coated IGU – SHGC of the electrochromic IGU in the bleached state) * 0.2*

where 0.712 quads is national energy consumption for the heating season
and 0.20 = estimated market penetration

The net energy savings and the reduction in carbon emissions for each scenario

[13] (a) Hill RJ, Nadel S.J *Coated Glass Applications and Markets*. Fairfield:,**1999**. (b) Andereck KJ Transforming Exterior Walls with Electrochromic Windows. *Environmental Design and Construction*, 2001. (WWW location: http://www.edcmag.com/CDA/ArticleInformation/features/BNP__Features__Item/0,4120,20035,00.html)

represented in Table 9 is given in Table 10 with the reduction in carbon emissions calculated as follows:

*(4) reduction in carbon emissions = net energy savings * 16.02 Kg/MMBtu*

where 16.02 Kg/MMBtu is the carbon emission factor for electricity

Table 10. Energy savings data for various electrochromic IGU configurations with and without low-E coatings included.

layer 1	layer 2	SHGC	relative net energy savings (quad)	relative reduction in C emissions (*10^6 MKg/yr)
clear	SB60 (R5)	0.465	0	0
EC Pane BLEACHED	clear	0.402	0.016	259
EC Pane TINTED	clear	0.305		
EC Pane BLEACHED	SB60 (R5)	0.290	0.022	355
EC Pane TINTED	SB60 (R5)	0.165		
EC Pane BLEACHED with SB60 (R4)	clear	0.255	0.020	328
EC Pane TINTED with SB60 (R4)	clear	0.144		
EC Pane BLEACHED	SB70XL (R5)	0.248	0.021	350
EC Pane TINTED	SB70XL (R5)	0.129		
EC Pane BLEACHED with SB70XL (R4)	clear	0.197	0.019	299
EC Pane TINTED with SB70XL (R4)	clear	0.103		

This electrochromic technology incorporated in an IGU does offer improved energy savings over that of a typical IGU of approximately **0.02 quad per year** with a reduction in C emissions for electricity of **259 MKg per year**. This value could increase to as much as **0.05 quad per year** with a reduction in C emissions for electricity of **801 MKg per year** if the heating penalty is removed which may be the case in southern climates or commercial structures where cooling is predominate year-round. However, further optimization of the system to improve the overall durability of the electrochromic technology would have to be made before the extent of any savings could be fully evaluated.

Subtask 4.7. Commercial manufacturing cost defensibly estimated to be less than $100 per square foot

A brainstorming session was held with PPG experts in IGU construction, and in the incorporation of electronics into IGUs and automotive windshields, to better understand a potential process to construct a dynamic IGU with this technology and the costs associated with such a process. The results of this session and subsequent follow-up were used to construct a more detailed process map (Figure 49) and a cost estimate for IGU manufacturing. The cost estimate has two extremes. The low end would include using $F:SnO_2$ as the TCO in the electrochromic cell and the high end includes the use of ITO as the TCO. Addition of the electrochromic to the IGU would increase the cost by 17 (low end) to 47 (high end) times the cost of a typical IGU.

There are several other considerations that will also have to be accounted for which are not included in the current cost estimate: licensing fee for use of ionic liquids in electrochromic devices and the development and fabrication of controllers. In addition, the following capital investments would be required: glass washing/rinsing line, two slot dye coaters with drying ovens, an electrodeposition chamber, a rinsing line, a drying oven, a vacuum filling line for ionic liquid laminant and an IGU assembly line.

We also discussed the potential market value of a fenestration product based on this technology with the PPG marketing team. Their input was that the technology would have to be laminated, and haze would need to be as low as possible. By controlling the cost and decreasing haze to less than 1 percent, the technology would open up to more applications. Specific comments made regarding the residential market were that the technology would most likely enter the market in specialty applications geared towards glare reduction such as sunrooms and skylights. In addition, for the exterior commercial market segment, addressable infrared attenuation may not be desirable due to cooling being the major energy consumable.

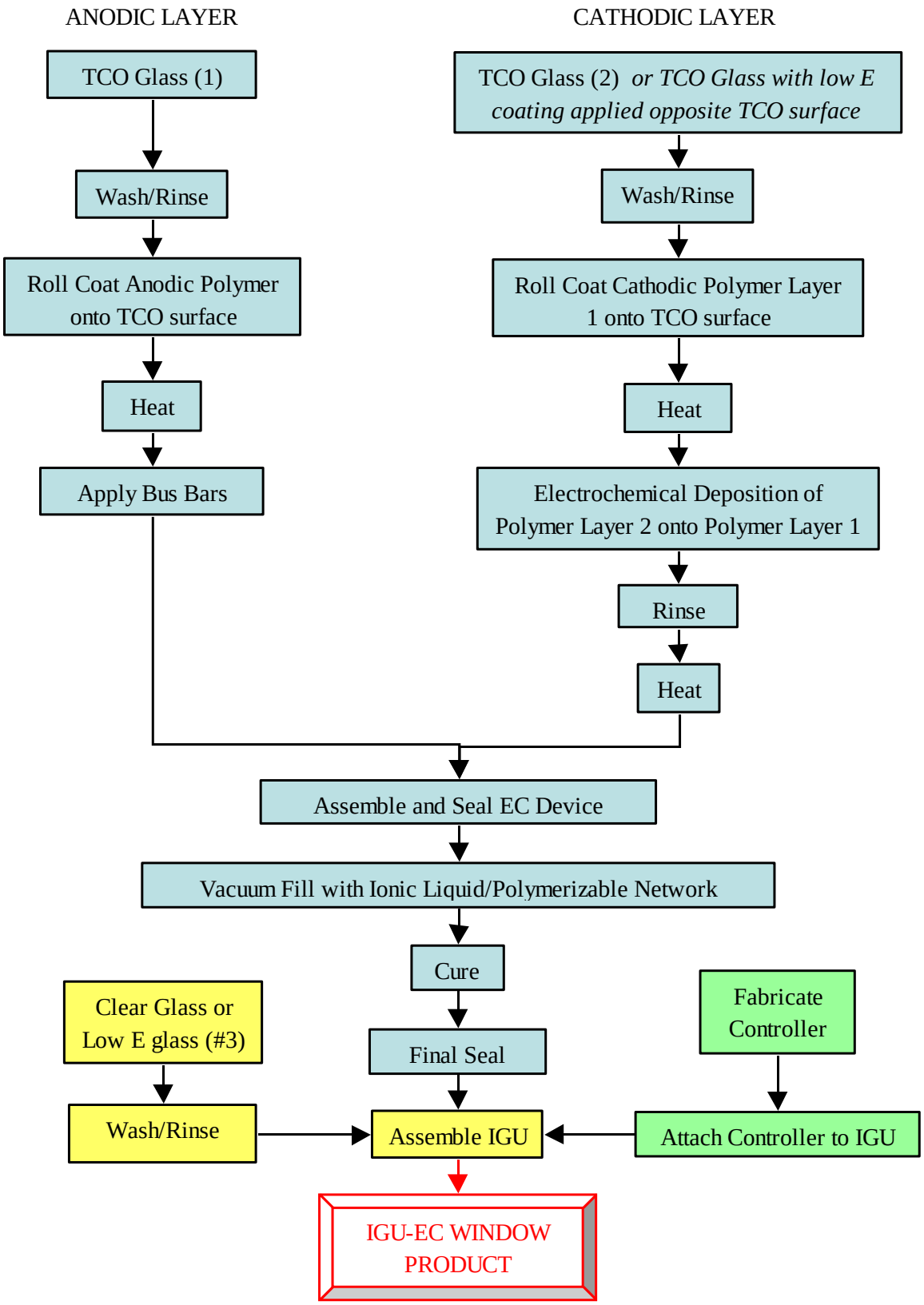

Figure 49. Process Map for Electrochromic Window Insulated Glass Unit Fabrication.

6. Identify products developed under the award and technology transfer activities such as:

a. Publications, conference papers, or other public releases of results.
none

b. Website or other Internet sites that reflect the results of this project.
none

c. Networks or collaborations fostered
The Principal Investigator and the PPG Glass Technology Center Consultant visited the University of Florida to discuss Professor John Reynolds' work in conducting polymer synthesis and characterization. We also initiated work with a specialty chemicals company to discuss UV protection and evaluated some of their conducting polymers that demonstrated infrared responsive behavior. Discussions were held with another company involving large-scale electrochemical deposition. Please contact Principal Investigator for additional information.

d. Technologies/techniques
none

e. Inventions/Patent Applications, licensing agreements
The following Memoranda of Invention was disclosed.

"Bilayer electrode for high-contrast electrochromic devices", disclosed by I. Schwendeman, 11/16/06.

f. Other products, such as data or databases, physical collections, audio or video, software, models, educational aid or curricula, instruments or equipment
none

7. For projects involving computer modeling, provide the following information:

a. Model description, key assumptions, version, source and intended use
WINDOW 5.2 is a publicly available computer program for calculating total window thermal performance indices (i.e. U-values, solar heat gain coefficients, shading coefficients, and visible transmittances). WINDOW 5.2 provides a versatile heat transfer analysis method consistent with the updated rating procedure developed by the National Fenestration Rating Council (NFRC) that is consistent with the ISO 15099 standard. The program can be used to design and develop new products, to assist educators in teaching heat transfer through windows, and to help public officials in developing building energy codes.[14]

[14] http://windows.lbl.gov/software/window/window.html

The version of the software that was used for this document was v5.2.17.

The software is available online at:
http://windows.lbl.gov/software/window/window.html.

For the work contained within this document, the software was used to estimate the surface temperatures of the glass in insulated glass units under NFRC 100-2001 summer conditions and to determine the U-value, solar heat gain coefficient, and visible transmittance for the glazing system (center-of-glass values).

b. Performance criteria for the model related to the intended use
see http://windows.lbl.gov/software/window/window.html

c. Test results to demonstrate the model performance criteria were met
see http://windows.lbl.gov/software/window/window.html

d. Theory behind the model, expressed in non-mathematical terms
see http://windows.lbl.gov/software/window/window.html

e. Mathematics to be used, including formulas and calculation methods
see http://windows.lbl.gov/software/window/window.html

f. Whether or not the theory and mathematical algorithms were peer reviewed, and if so, include a summary of theoretical strengths and weaknesses
The program is consistent with the updated rating procedure of the NFRC and the ISO 15099 standard. See http://windows.lbl.gov/software/window/window.html for information regarding the theoretical strengths and weaknesses.

g. Hardware requirements
Hard disk drive with at least 150 MB of available disk space is required. The program has been tested on Microsoft Windows XP and Windows 2000™. Older versions of Microsoft Windows might work, but are not supported. (The program WILL NOT run with Windows 3.1™, Windows NT 3.51™ or Windows 95™).

WINDOW has been tested and run successfully on Apple computers with Intel processors by using Parallels Desktop 3.0 for Mac. This software allows you to install Windows XP or Windows Vista on your Mac, and you can install our software in that version of Windows XP or Vista. See www.parallels.com for more information.

h. Documentation (e.g., users guide, model code)
see http://windows.lbl.gov/software/window/window.html

APPENDIX

$BMIM\text{-}BF_4$	1-butyl-3-methylimidaolium tetrafluoroborate
E_h	hemispherical emissivity
EDOT	2,3-dihydrothieno[3,4-b]-1,4-dioxin
$F:SnO_2$	fluorine doped tin oxide
IGU	insulated glass unit
IR	infrared
ITO	tin doped indium oxide
LBNL	Lawrence Berkley National Laboratory
low-E	low emissivity
MAF-15	experimental monomer, 3,4-(2',2'-dimethylpropylene)-dioxythiophene
MAF-17	experimental monomer
MSVD	magnetron sputtering vapor deposition
NIR	near infrared region of the solar spectrum (800-1200 nm)
OSCP	organic semiconducting polymer
PANI	polyaniline
PEDOT	poly(2,3-dihydrothieno[3,4-b]-1,4-dioxin)
PMAF-15	poly(3,4-(2',2'-dimethylpropylene)-dioxythiophene)
POT	poly(3-octylthiophene-2,5-diyl)
PPG	PPG Industries
PTR	photopic transmittance ratio
PVDF	poly(vinyladine fluoride)
R_s	sheet resistance
RTIL	room temperature ionic liquid
SB60	Solarban® 60 low-E coated glass
SB70XL	Solarban® 70XL low-E coated glass
SFST	Santa Fe Science and Technology
SHGC	solar heat gain coefficient
TBAP	tetrabutyl ammonium perchlorate
TCO	transparent conductive oxide
UV	ultraviolet region of the solar spectrum (<400 nm)
VIS	visible region of the solar spectrum (400-800 nm)
WO_3	tungsten oxide
XRD	x-ray diffraction
XRF	x-ray fluorescence